Available online at www.CivileJournal.org

Civil Engineering Journal

(E-ISSN: 2476-3055; ISSN: 2676-6957)

Vol. 12, No. 05, May, 2026

Damage-Aid Alignment and Reconstruction Pace Diagnostics for Post-Earthquake Recovery

Evrim Oyguc [1], Resat Oyguc [1*]

[1] *Department of Earthquake Engineering, Institute of Disaster Management, Istanbul Technical University, Istanbul 34469, Turkey.*

Received 02 January 2026; Revised 23 April 2026; Accepted 29 April 2026; Published 01 May 2026

Abstract

Post-earthquake reconstruction raises two governance questions that are rarely addressed jointly. Whether affected provinces receive allocations proportional to measured damage, and whether physical delivery keeps pace with official plans, remain open in the empirical literature. This study addresses both the 2023 Kahramanmaraş sequence, which affected eleven Turkish provinces and generated recovery needs of approximately USD 103.6 billion. Two rule-based diagnostics are specified, the Damage–Aid Alignment index, which combines Spearman rank correlation with Theil T divergence, and the Reconstruction Pace Index, a monthly delivery-to-plan rate governed by a pre-specified run rule. Both diagnostics operate on an author-compiled corpus of 15,928 building-level records aggregated to a province–month panel spanning March 2023 to August 2024 and cross-checked against independent remote-sensing products. A two-way fixed-effects panel regression complements the analysis. Alignment with need is strong, with a Spearman correlation of 0.836 and a Theil T of 0.087, though Hatay is over-allocated by 10.4 percentage points and Adıyaman is under-allocated by 6.0. Persistent pace shortfalls in three provinces are clear within two months and reflect mobilization frictions rather than systemic failure. The framework provides a low-friction, auditable pathway to routine post-disaster performance monitoring.

Keywords: Post-Earthquake Recovery; Housing Reconstruction; Disaster Recovery Governance; Build Back Better; Damage-Aid Alignment.

1. Introduction

On 6 February 2023, a doublet of major earthquakes struck southeastern Türkiye in rapid succession. The first mainshock, with a moment magnitude of M_w 7.7, ruptured near Pazarcık at 04:17 local time. A second event of M_w 7.6 followed within nine hours along the Çardak–Sürgü system, and a further M_w 6.4 earthquake struck near Yayladağı on 20 February [1]. Ground-motion records from the Disaster and Emergency Management Presidency (AFAD) network document peak ground accelerations between 0.5 g and 1.0 g at many stations, reaching 2.2 g near the primary rupture zone [1]. Over the 0.5–1.0 s period range critical for the prevailing regional building stock, spectral accelerations exceeded the design-basis thresholds of the Turkish Building Earthquake Code [2] and, at several stations, surpassed the Maximum Considered Earthquake level, helping to explain both the breadth and the severity of the urban damage that followed.

The destruction was spatially extensive. AFAD formally designated an affected zone exceeding 190,000 km² with approximately 18 million residents, and roughly 260,000 structures were classified as severely damaged or destroyed [1]. Hatay, Kahramanmaraş, Malatya and Adıyaman bore the heaviest structural losses. The scale of destruction reflects the combination of measured shaking and pre-existing vulnerabilities in the regional building stock, which naturally motivates an urban and governance-aware reading of the event, since damage to the built environment and critical urban infrastructure is translated into recovery and planning decisions through administrative processes and constraints [3].

* Corresponding author: oyguc@itu.edu.tr

https://doi.org/10.28991/CEJ-2026-012-05-022

© 2026 by the authors. Licensee C.E.J, Tehran, Iran. This article is an open access article distributed under the terms and conditions of the Creative Commons Attribution (CC-BY) license (http://creativecommons.org/licenses/by/4.0/).

Establishing the physical footprint of the sequence drew on an unusually rich convergence of sources. Independent finite-fault inversions and Interferometric Synthetic Aperture Radar (InSAR)-assisted kinematic models resolved the multi-segment rupture geometry and slip distribution [4–9]. Copernicus Emergency Management Service (CEMS) graded-damage products [10] and NASA Advanced Rapid Imaging and Analysis (ARIA) coherence and displacement fields [11, 12] provided near-continuous spatial coverage through successive acquisition windows, complemented by independent post-event damage assessments from SAR and optical imagery [13] and hybrid damage-detection techniques combining multi-temporal coherence and amplitude [14]. AFAD's administrative building-tagging system generated the earliest district-level severity estimates. Provisional map editions were time-stamped and versioned, accompanied by uncertainty notes, and reconciled against field inspections and ministry tallies before aggregation to district and province. Damage information from strong-motion records, CEMS products, and ARIA coherence and displacement outputs were integrated into a rapid damage-information pipeline that routed validated signals to search, lifeline, and settlement decisions. Figure 1 summarizes the sequence.

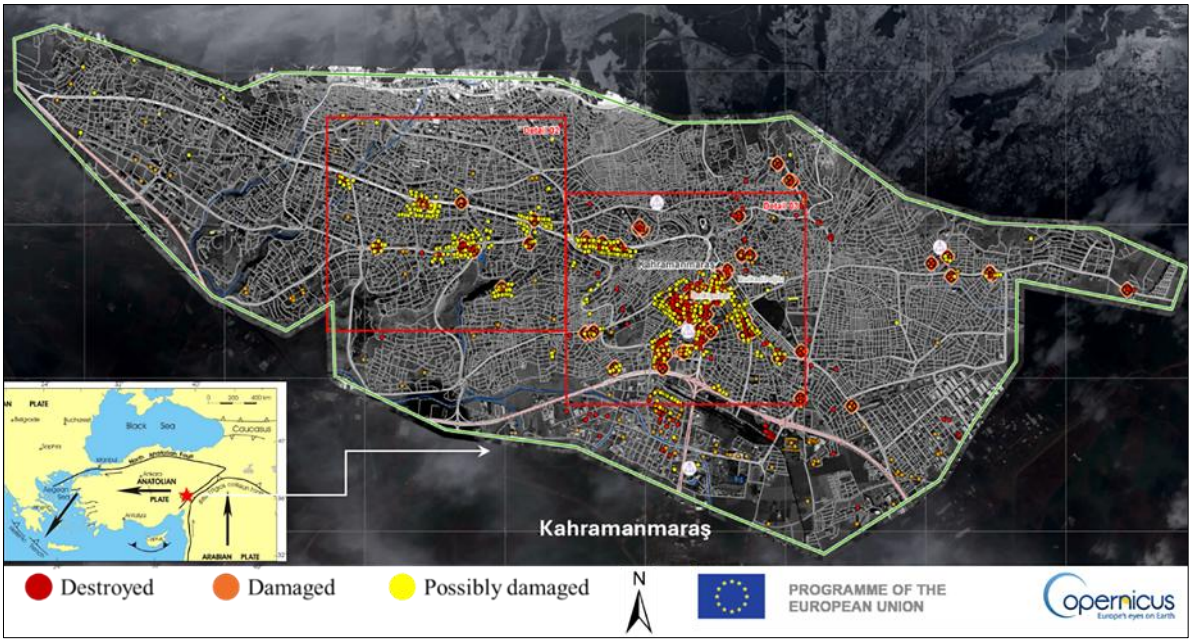

Figure 1. Rapid damage-information pipeline in the first fortnight: administrative inspections, CEMS graded damage, and ARIA coherence/displacement products feeding search, lifeline, and settlement tasking [12]

At the macroeconomic level, housing dominated the total impact, accounting for 54.9% of losses (TRY 1,073.9 billion), followed by public infrastructure and service buildings (TRY 242.5 billion) and private non-housing assets (TRY 222.4 billion). The total macroeconomic effect is approximately 9% of 2023 national income. Complementary government tables indicate TRY 1,139.7 billion, or about 4.47 % of GDP, allocated in 2023 across central and local budgets and dedicated funds [15]. The Türkiye Earthquakes Recovery and Reconstruction Assessment (TERRA) [15] placed total recovery and reconstruction needs at approximately USD 103.6 billion, clarifying the order of magnitude of resources and timelines implied by the built-environment recovery task. Table 1 benchmarks the event against selected historical earthquakes; the estimated loss is broadly comparable to Sichuan (2008) and below Tohoku (2011), placing the 2023 Türkiye sequence among the largest post-earthquake reconstruction tasks of the past two decades. A task of this magnitude sharpens a long-standing but unresolved question in the literature, namely, how post-disaster recovery can be monitored, audited, and governed as a routine public output rather than as a retrospective narrative.

Table 1. Benchmarking direct economic loss (historic cost) for selected earthquakes [15]

Event	Location	Magnitude (M_w)	Historic cost (billion)
2011 Tohoku earthquake	Japan	9.0	USD 360
2023 Kahramanmaraş earthquakes	Türkiye	7.8 & 7.7	USD 163.3
2008 Sichuan earthquake	China	7.9	USD 130
2004 Chuetsu earthquake	Japan	6.6	USD 28
2010 Canterbury & 2011 Christchurch earthquake	New Zealand	7.0 & 6.2	USD 27
2016 Kumamoto earthquakes	Japan	7.0	USD 25
2011 Sikkim earthquake	India	6.9	USD 22.3
2009 L'Aquila earthquake	Italy	6.3	USD 16
2012 Northern Italy earthquakes	Italy	6.1	USD 15.8
2010 Chile earthquake	Chile	8.8	USD 15

A substantial literature has addressed aspects of this question, and it is helpful to organize existing contributions into three thematic strands that are individually mature but collectively fragmented. A first strand concerns post-disaster loss and needs assessment, where standardized protocols such as the Post-Disaster Needs Assessment framework and the Global Rapid Post-Disaster Damage Estimation methodology translate physical damage into monetary estimates and reconstruction requirements within days of an event [15, 16]. A second strand focuses on the development of recovery indicators and monitoring frameworks, beginning with early satellite-assisted efforts to track physical rebuilding [17] and extending to more recent multi-sector indicator systems designed for post-disaster community recovery at municipal and regional scales [18]. A third strand tracks reconstruction itself through Earth observation, using SAR coherence, optical change detection, and night-time light trajectories to generate spatially continuous signals of rebuilding progress [11, 19-21]. Complementing these three strands, separate project-management literature has shown that schedule slippage, procurement friction, and multi-actor coordination failures are systematic rather than exceptional features of post-disaster reconstruction [22, 23].

Despite the maturity of each individual strand, three gaps persist that are directly relevant to the present study. First, standardized loss assessments quantify aggregate need at a national or regional scale but are rarely extended to province-level delivery monitoring over time, and they do not report proportionality statistics that would allow allocations to be read against measured need at intermediate resolution. Second, recovery-indicator frameworks [18] typically report status variables without operationalizing pre-specified thresholds that would distinguish persistent under-delivery from transient fluctuation, and they are seldom anchored to the statutory municipal workflows through which reconstruction is legally executed. Third, Earth-observation monitoring generates high-resolution physical signals that are rarely coupled with administrative reporting ledgers so that physical progress and legal-administrative performance are tracked in parallel rather than jointly.

Comparative post-disaster studies have repeatedly demonstrated the central role of institutional arrangements in shaping recovery outcomes, from the Canterbury earthquakes [24] and the Great East Japan earthquake and tsunami [25] to earlier reconstruction programs in Türkiye [26, 27], yet such comparative insights have seldom been translated into diagnostic tools that municipalities can operate on their own data. The implication is that equity and pace, the two most visible dimensions of recovery performance, are typically reported retrospectively rather than monitored continuously. This study is positioned at the intersection of the three strands and is designed to address each of the three gaps directly. Equity is operationalized through the Damage–Aid Alignment (DAA) index, which reads proportionality between population-normalized damage and recorded allocations through the joint application of Spearman's rank correlation and the Theil T divergence. The two statistics are selected for their complementary properties, with the rank correlation capturing monotonic association and the Theil T quantifying deviation from strict proportionality and decomposing into interpretable components. Pace is operationalized through the Reconstruction Pace Index (RPI), a delivery-to-plan ratio computed at province–month resolution and governed by a pre-specified run rule that flags persistent rather than transient shortfalls, following established principles from statistical quality control [28].

Both diagnostics are constructed from routinely produced administrative ledgers, interpreted against the statutory municipal sequence of siting, plan revision, permitting, inspection, and energization, and complemented by a two-way fixed-effects panel regression that conditions the pace trajectory on observable provincial characteristics. Province-by-month resolution is adopted since it aligns with budgeting and accountability cycles, captures one full annual cycle of construction and administrative activity, and is sufficiently long for the run rule to distinguish sustained shortfalls from seasonal variation. An author-compiled, harmonized building-level dataset of 15,928 records underpins all estimates and is cross-checked against independent Earth-observation products to guard against systematic under-recording.

Against this backdrop, three interrelated questions guide the analysis. The first concerns the operationalization of equity as a measurable and auditable property of resource allocation at intermediate spatial scales. The second concerns the measurement of pace as a time-varying delivery-to-plan process capable of separating persistent structural shortfalls from mobilization-phase frictions. The third concerns the conditioning role of the municipal workflow, specifically whether the gates of siting, plan revision, permitting, inspection, and energization can be shown empirically to shape observed recovery outcomes. These questions are posed jointly since equity, pace, and governance are empirically coupled in the field. A province may be over-allocated relative to measured need yet deliver slowly as a result of inspection bottlenecks, and another may be under-allocated yet recover quickly on account of compact portfolio composition. Such interactions are invisible to any single-dimensional indicator and motivate the joint diagnostic design adopted here.

Institutional coordination was organized under the Türkiye Disaster Response Plan (TAMP) [29], through which AFAD's national lead role and inter-ministerial and municipal interfaces were defined across search and rescue, lifeline restoration, settlement siting, and reconstruction permitting. The same architecture was carried into the first year of recovery and was reflected in official summaries and technical notes prepared for donors and financial institutions. Since the stages through which reconstruction moves are municipal and procedurally codified, performance can be evaluated against a legal baseline rather than an informal one, a feature that makes the proposed diagnostics applicable beyond this event.

1.1. Seismotectonic of Southeastern Türkiye

Post-disaster management in the corridor is read from rupture mechanics to urban exposure and, finally, to the statutes that determine where and how rebuilding proceeds. Geophysical reconstructions explain corridor-wide lifeline failures, and Turkish disaster and municipal law determine whether reconstruction reduces rather than reproduces risk, focusing analysis on the city-scale levers of zoning, permitting, inspection, and urban transformation [30–38].

Recent kinematic reconstructions show a multi-segment rupture with rapid transfers between fault strands, consistent with the unusually broad footprints observed across provincial capitals and corridor towns [4–9]. The implication for recovery is practical: service interruptions and damage patterns propagate along segments and junctions, so siting, plan revision, permitting, and inspection must reference segment-level hazard and be resourced to keep delivery pace aligned with code compliance. Figure 2 locates the February 2023 doublet within this segmented system, organized into two principal strands. The main strand runs from the Amanos and Pazarcık segments into Erkenek; a northern strand follows Sürgü–Çardak through Pütürge and Palu toward the Karlıova junction.

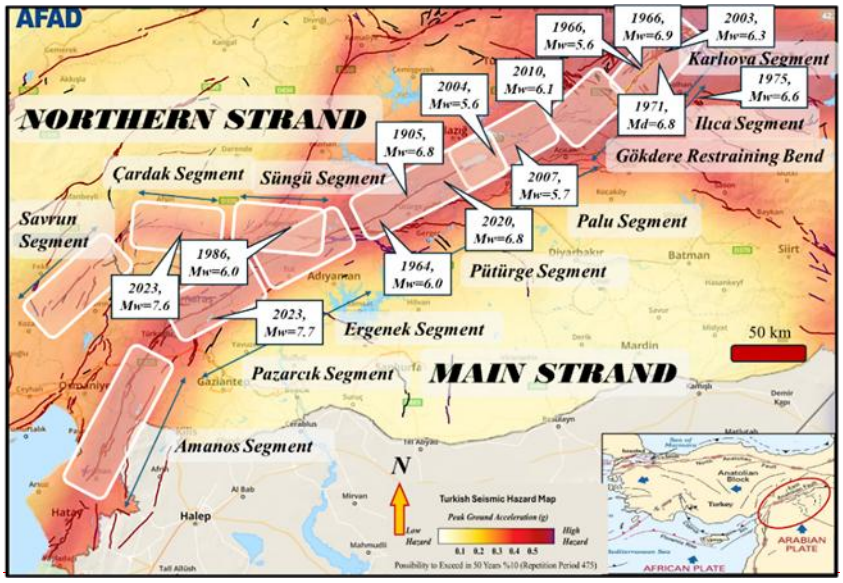

Figure 2. Tectonic segmentation of the EAF system showing the northern and main strands, along with major historical and recent earthquake ruptures

The first mainshock (M_w 7.7) ruptured primarily along Pazarcık on the main strand; the second mainshock (M_w 7.6) activated the Çardak–Sürgü system on the northern strand [6, 8]. Alternative moment-magnitude formulations, including corridor-specific scales such as M_{wg}, have been proposed in the seismological literature, but M_w values reported by AFAD and global catalogues are retained here since they constitute the official reference for the 2023 sequence and the diagnostics developed in this study depend on observed damage and recovery trajectories rather than on fine distinctions between magnitude scales. Rectangles delineate the approximate rupture zones for the 2023 events. Mapped surface ruptures and their approximate lengths along these segments are documented in detail by Emre et al. [39], to whom readers are referred for a full account of the 2023 rupture geometry.

Historical events distributed by segments reveal a corridor with the capacity for multi-fault sequences. The Pütürge and Palu segments have hosted twentieth- and twenty-first-century earthquakes at $M_w \geqslant 6$ (e.g., the 2020 Elazığ–Sivrice event on Pütürge [39]), while activity near Ilıca and Karlıova marks the northeastern continuation toward the triple-fault junction. This spatial mosaic implies stress accumulation and release distributed across multiple segments and structural bends, including the Gökdere restraining bend, rather than concentrated at a single repeating asperity [40].

1.2. Disaster Governance and Legal Frameworks

Türkiye's disaster governance is statute-based and nationally led. The framework is anchored in the Construction Zoning Law [41], the Building Inspection Law [42], the Municipal and Metropolitan Municipality Laws [43, 44], and Law 6306 on transformation [45], with post-February 2023 amendments updating siting, expropriation, permitting, and inspection powers at a municipal scale. Law No. 5902 [46] created AFAD and centralized strategic coordination through provincial branches and sectoral mandates; AFAD's own materials and legal summaries trace this architecture and its post-2017 placement under the Ministry of Interior. Within this architecture, TAMP [29] specifies the operating procedures for sheltering, debris clearance, lifeline restoration, and health and information management and governs how external support is integrated during surge and recovery phases.

Municipal authority becomes decisive in reconstruction. Municipal Law No. 5393 [43] and Metropolitan Municipality Law No. 5216 [44] assign corporate status, competences, finance, and, crucially, plan-making and service-delivery powers that determine whether risk-informed choices can be enforced [47]. Authoritative sources reproduce the key provisions, including Article 73 of Law 5393 on declaring urban transformation and development project areas and metropolitan jurisdiction over multi-district infrastructure and approvals under Law 5216. Where these powers are exercised in an integrated sequence (designation, plan revision, permit issuance, inspection, and energization), reconstruction quality and delivery pace reinforce each other. Where any step is decoupled, delivery may accelerate on paper while structural risk accumulates undetected [48–56].

Build Back Better (BBB) operates as an enforceable municipal program when siting, plan revision, permitting, and inspection are sequenced and measurable, so delivery pace and quality reinforce rather than erode one another. The Disaster Recovery Framework Guide [57] articulates pre-arranged recovery institutions, risk-informed land use and siting, enforceable inspection, continuity planning for lifelines, and financing instruments that preserve quality under political pressure; UNDRR materials on Priority 4 of the Sendai Framework reinforce this agenda and stress readiness for recovery as a standing capability [58, 59].

These powers operate within the national Zoning Law No. 3194 [41], which governs plan hierarchies, land-use regulation, and building permissions and are complemented by Building Inspection Law No. 4708 [42], which regulates independent inspection companies and the sequencing of construction controls. The comparative governance literature and official summaries converge on a basic finding: plans and codes are necessary but not sufficient; performance in spatially extensive crises turns on rehearsed interoperability, clear delegation to municipalities, and timely situational awareness flowing from periphery to center.

Figure 3 consolidates the statutory architecture and groups instruments by function rather than by ministry. Codes translate hazard into enforceable design and inspection requirements. Zoning and land-use statutes govern where density and use may shift. Municipal laws define who can designate areas, revise plans, and issue permits. Heritage law constrains protected settings, and housing and development statutes shape program delivery. Within this architecture, reconstruction is typically operationalized through policy choices among preservation, rehabilitation, and redevelopment pathways, selected in relation to the character of destruction and the values intended to be retained [60].

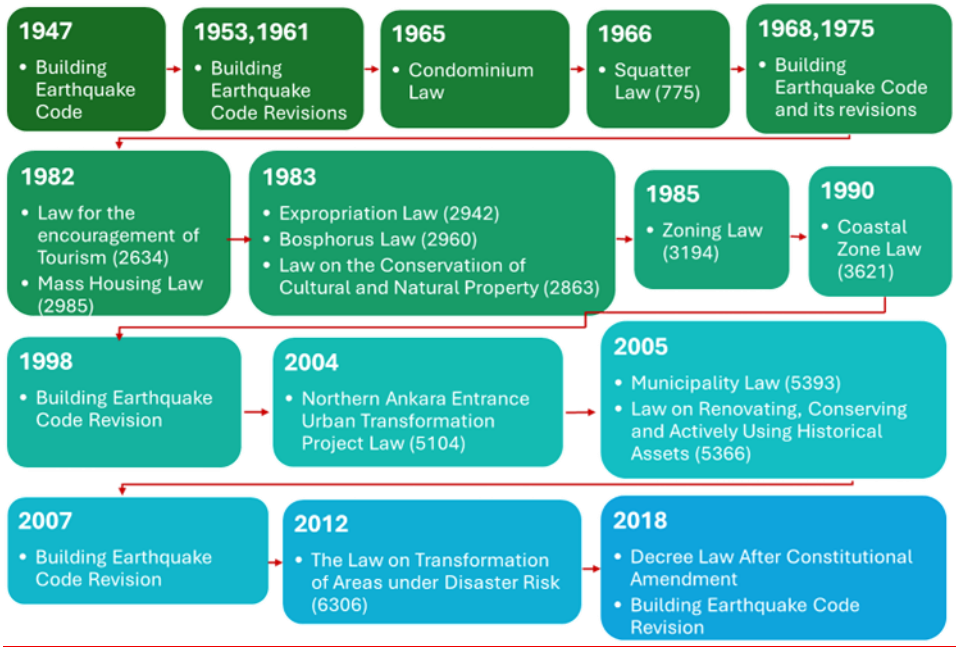

Figure 3. Urban transformation legislation in Türkiye: A visual representation of key legal frameworks

Plan law covers siting and plan revision; the code governs permits and inspections; municipal powers mediate program speed; the inspection regime safeguards quality; and heritage law constrains form and façade in designated landscapes. This functional reading also clarifies why pace and quality rise or fall together. When parcel designation, plan revision, permitting, and inspection run as a sequenced municipal workflow, output and compliance reinforce each other. When any step is decoupled, delivery may accelerate on paper while risk quietly accumulates [48–56]. The overall structure of this governance and diagnostic system is synthesized in Figure 4, which places the Damage–Aid Alignment index and the Reconstruction Pace Index within the statutory disaster governance framework and the municipal gates that condition recovery outcomes.

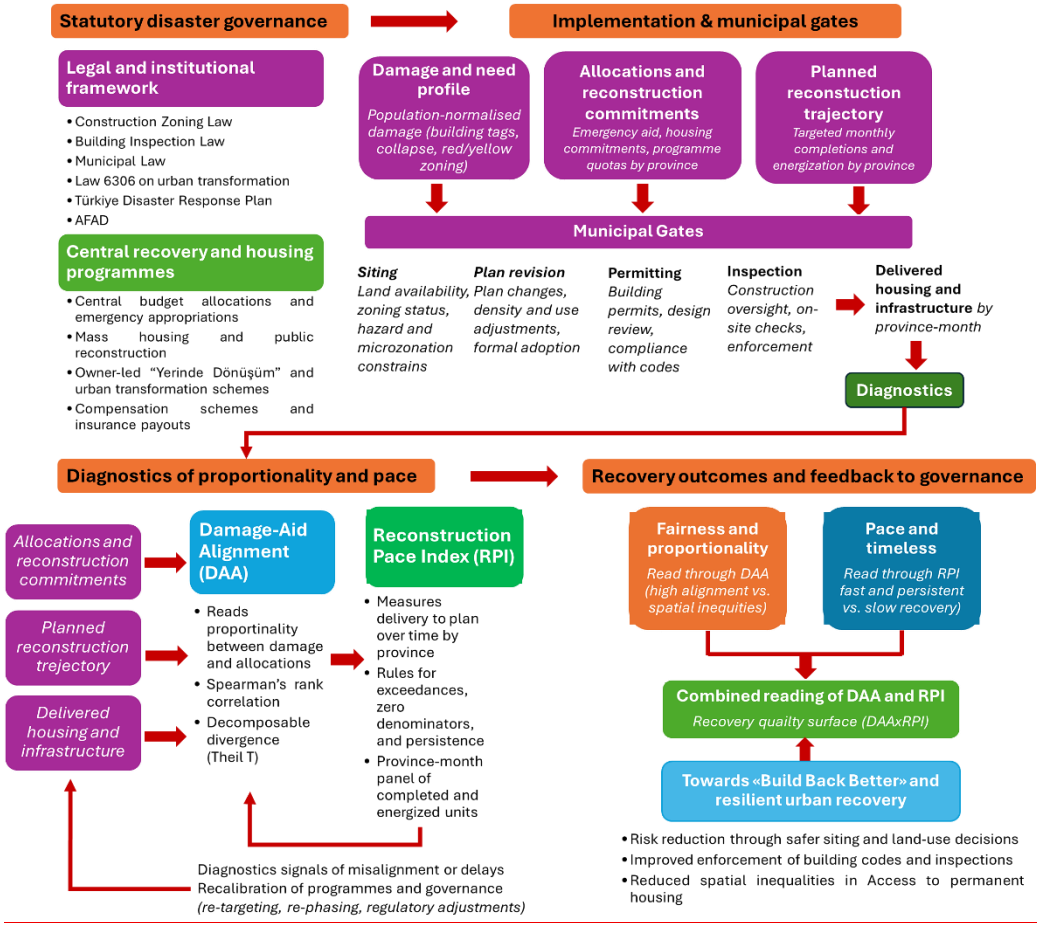

Figure 4. Conceptual framework linking statutory disaster governance, the DAA and RPI diagnostics, and recovery outcomes through municipal gates

1.3. Contribution and Organization of the Paper

Four contributions are offered. First, a harmonized, author-compiled, building-level corpus of 15,928 records is produced and translated into a province–month panel that aligns with budgeting and accountability cycles. Second, rule-based diagnostics (DAA and RPI) are specified in advance, and handling conventions for exceedances, zero-denominator months, and persistence are stated so that the same rules can be applied by others. Third, uncertainty is reported in a form that is compatible with routine disclosure rather than with one-off academic reporting, using nonparametric bootstrap at the province level and Wilson intervals for finite-sample proportions. Fourth, portfolio composition across dwellings, commercial premises, and barns is summarized through Jensen–Shannon divergence and a log–log scale relation, and the results are interpreted by program mix, as the mix is shown to shape the administrative burden faced during implementation.

The remainder of the paper is organized as follows. Section 2 presents the methods and diagnostic framework, covering the study area, the author-compiled corpus and its harmonization, the Damage–Aid Alignment and Reconstruction Pace Index specifications, the compositional analysis framework, and the panel econometric strategy. Section 3 reports sample-based severity diagnostics, the province-level DAA values, province–month RPI trajectories, panel regression estimates, and the provincial entitlement register. Section 4 discusses the findings, synthesizes the governance implications, and offers a structured comparison with prior studies. Section 5 concludes with the limits of the design and directions for further work.

2. Methods and Diagnostics

The empirical design combines geospatial change detection with documentary and legal analysis, compact panel econometrics, and compositional inquiry. Each strand is specified to permit replication, with crosswalks between administrative tallies of building damage, earth-observation layers, population denominators, and dated records of housing delivery. This architecture supports two central diagnostics, the Damage–Aid Alignment (DAA) index and the Reconstruction Pace Index (RPI), and frames their interpretation against municipal instruments that govern plan revision, siting, permitting, and inspection in Türkiye.

Throughout the methodological exposition, the province index is denoted i with i = 1, …, n, where n = 11; the month index is denoted t; and all summations run over the relevant index unless stated otherwise. Damage counts are denoted

C_i, U_i, and H_i for collapsed, urgently demolishable, and heavily damaged buildings, respectively; Pop_i denotes the resident population of province i from the pre-event register; D_i, C_i, and B_i denote observed damaged dwellings, commercial premises, and barns in the author-compiled corpus; $S_i = D_i + C_i + B_i$ denotes the corresponding provincial sample total. Share notation follows the convention that s_i^{need} and s_i^{alloc} denote need and allocation shares, that pi^D, pi^c, and pi^B denote within-province simplex compositions, and that $Alloc_i$ denotes the allocation volume of aid or housing units for province i. Inferential statistics follow the convention that ρ_s denotes Spearman's rank correlation, T denotes the Theil divergence, β denotes regression slope coefficients, α_i and γ_t denote province and month fixed effects, and ε_{it} denotes the idiosyncratic error term.

2.1. Affected Provinces and Case Selection

The earthquake sequence directly affected eleven provinces formally recognized in national notices and operational briefs, with subsequent determinations extending general life-affecting disaster area status to additional localities where damage tallies warranted inclusion [1]. Provincial capitals and major districts in Kahramanmaraş, Hatay and Adıyaman serve here as primary cases for close analysis, with Gaziantep and Malatya used for cross-checks on exposure and reconstruction delivery. Case cities were selected by three transparent criteria: (i) a share of severely damaged buildings above the provincial median during the first administrative sweep; (ii) documented lifeline interruptions within the first fortnight; and (iii) availability of consistent administrative reporting for ≥ 12 consecutive months. The requirement of at least twelve consecutive months of reporting ensures that the resulting province–month series spans the transition from emergency response to early reconstruction, captures one full annual cycle in construction and administrative activity, and provides a sufficiently long trajectory for the persistence rule in the Reconstruction Pace Index to distinguish sustained shortfalls from short-lived fluctuations. All eleven designated provinces satisfied all three criteria and are therefore included in the full panel.

Official communications by AFAD set the administrative perimeter of the disaster zone [1], and partner summaries document the population scale and institutional implications of these designations, including the initial period of state of emergency and the activation of extraordinary siting and permitting powers for recovery [61]. Figure 5 provides an administrative-scale portrait of the study area: Kahramanmaraş is depicted at the center of a stylized epicentral field, and the surrounding provinces of Hatay, Osmaniye, Adana, Gaziantep, Kilis, Adıyaman, Malatya, Elazığ, Diyarbakır and Şanlıurfa extend across the damage footprint in both directions along the fault system, with exposure declining systematically with distance from the primary rupture traces.

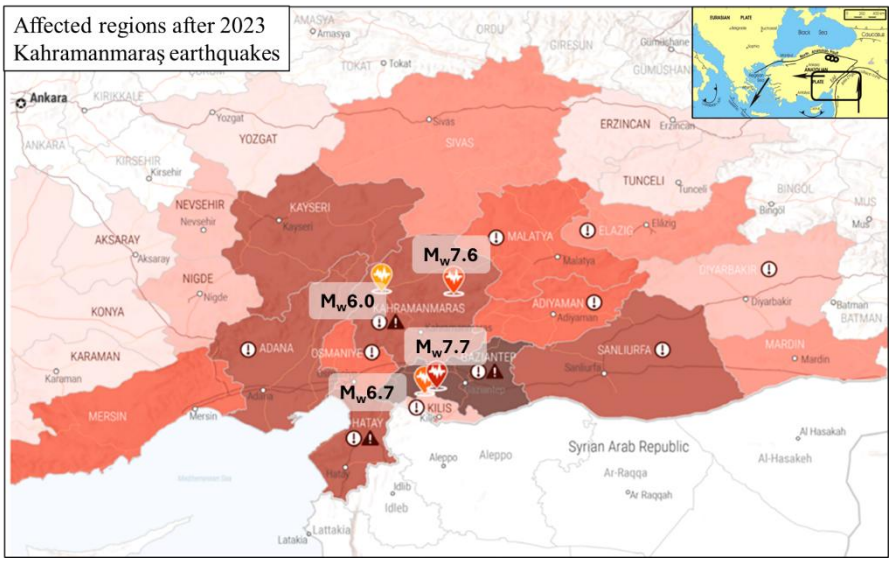

Figure 5. Affected provinces after the 2023 Kahramanmaraş earthquakes

2.2. Data Sources and Harmonization

Two scales of evidence are used for different analytical purposes throughout the paper. Official national aggregates from the Türkiye Earthquakes Recovery and Reconstruction Assessment establish the overall magnitude and sectoral composition of damage and anchor the macroeconomic framing [15]. In parallel, an author-compiled, building-level corpus of 15,928 records, harmonized with administrative damage categories and aggregated to a province–month panel, underpins the governance diagnostics and the panel regression. Cross-checks against Copernicus EMSR648 graded-damage extents [10] and NASA ARIA displacement products [11, 12] serve as external validity constraints on the administrative series, with complementary benchmarks available from independent SAR and optical post-event analyses [13, 62, 63] and from ground-deformation studies using Sentinel-2 imagery [64].

2.2.1. Author-Compiled Building-Level Corpus

The author-compiled corpus was constructed from three primary sources accessed between March 2023 and February 2024: (i) building damage determinations issued by the Ministry of Environment, Urbanization and Climate Change (MEUCC) through the national Damage Assessment Inquiry portal; (ii) humanitarian aggregation products that compiled MEUCC classifications at the mahalle (neighborhood) scale and made them accessible through inter-agency reporting channels [61]; and (iii) two additional administrative datasets cross-referencing entitlement adjudications against georeferenced parcel identifiers. Each record carries an asset-class label (dwelling, commercial premise, or barn), a damage category (collapsed, urgently demolishable, or heavily damaged), and a province identifier.

Harmonization proceeded in three steps. First, damage categories were mapped to the administrative taxonomy used in the national entitlement system; records that could not be unambiguously assigned were excluded rather than reclassified. Second, asset-class labels were standardized across sources, with ambiguous cases adjudicated by reference to the parcel-use register. Third, records were aggregated to province–month cells, with the date of the administrative determination taken as the time stamp, with appeals and revisions incorporated at the month of the revised determination. The resulting panel is an observed sample drawn from the universe of administrative records, not a census. All estimates are interpreted strictly within this sample frame.

Table 2 summarizes the corpus by province and asset class. Damage is heavily concentrated: Hatay, Kahramanmaraş, Malatya, and Adıyaman together account for approximately 79% of all 15,928 records, with Hatay alone representing 37.5% of the sample. Dwellings account for 68.9 % of records (10,974 units), commercial premises for 27.4 % (4,357), and barns for 3.7 % (597). The asset composition carries direct operational significance: Elazığ and Kilis hold disproportionately high barn shares relative to their total sample size, indicating rural-livelihood exposure that extends beyond the housing program; by contrast, Adana presents a predominantly urban profile with barn losses below 1.5% of its provincial total.

Table 2. Author-compiled building-level corpus by province and asset class; counts cover buildings classified as heavily damaged, urgently demolishable, or collapsed (total records = 15,928)

Province	Dwellings	Commercial premises	Barns	Total
Hatay	4,108	1,676	188	5,972
Kahramanmaraş	1,823	779	78	2,680
Malatya	1,687	674	98	2,459
Adıyaman	1,064	333	69	1,466
Gaziantep	691	442	58	1,191
Osmaniye	333	126	6	465
Elazığ	325	77	49	451
Diyarbakır	349	79	21	449
Şanlıurfa	278	101	18	397
Adana	261	60	4	325
Kilis	55	10	8	73
Total	**10,974**	**4,357**	**597**	**15,928**

The representativeness of the corpus relative to the full affected building stock warrants explicit discussion, and the design response is best described as a triangulation across three complementary data layers rather than reliance on any single source. Administrative tallies produced by AFAD and summarized in the Türkiye Earthquakes Recovery and Reconstruction Assessment record approximately 260,000 buildings classified as severely damaged or destroyed across the eleven provinces, while the entitlement register adjudicated by mid-January 2024 comprises 387,776 dwellings, 40,422 workplaces, and 11,424 barns for a total of 439,622 accepted entitlements. The author-compiled corpus of 15,928 records is therefore an observed sample drawn from these larger administrative universes rather than a census of affected buildings, and it is restricted to buildings classified as heavily damaged, urgently demolishable, or collapsed, in line with the severity categories used in the Damage Severity Index.

Three indicators support the interpretation that the corpus captures the underlying structure of severe damage at the province scale despite its partial coverage. Spatial concordance is the first: when provincial shares in the corpus are compared with provincial shares in the entitlement register, the Spearman rank correlation between the two distributions is 0.955 across the eleven provinces, and the provincial share differs by less than three percentage points for nine of the eleven provinces, with the two remaining cases (Hatay at +2.9 and Gaziantep at +2.9 percentage points relative to the entitlement share) reflecting the geographic concentration of the initial fieldwork on the heaviest-damage corridor. The four leading provinces in terms of absolute severe-damage counts are the same in both sources, although the relative

ordering between Malatya and Kahramanmaraş within this leading group reverses between the two accounts, reflecting differences in the timing of appeals closure rather than a systematic bias in the corpus. External verification is the second: the corpus has been cross-checked against Copernicus EMSR648 graded-damage extents and NASA ARIA displacement and damage-proxy products, with agreement reported as high in the four most affected provinces and with divergences in peripheral areas handled by flagging rather than substitution. Internal uncertainty propagation closes the set: compositional statistics computed on the corpus are accompanied by Wilson 95% confidence intervals, which translate finite-sample size directly into reported interval widths and prevent the partial coverage from being absorbed silently into point estimates.

The analytical division of labor among the three data layers is important to the representativeness question. Damage–Aid Alignment statistics are computed from MEUCC administrative counts and from the official entitlement register and therefore rest on the full administrative universes rather than on the 15,928-record sample. The corpus is used in the compositional analysis in Section 3.1, where a joint breakdown across dwellings, commercial premises, and barns is required at province resolution and where such a joint breakdown is not consistently available in the publicly released aggregated administrative tables at sub-district spatial resolution. Panel regression draws on the province–month delivery and plan series from the rolling official plan and on province-level characteristics that are stable under the corpus sample. Representativeness of the corpus is therefore consequential for the compositional layer of the analysis, where uncertainty is explicitly propagated through Wilson intervals and is not a binding constraint on the alignment and pace diagnostics, which are anchored to administrative universes. The triangulation among MEUCC counts, the author-compiled corpus, and the Earth-observation products is the design choice that absorbs the representativeness question at the point at which it arises in each analytical layer, rather than resolving it in a single summary table.

2.2.2. Remote Sensing and Population Denominators

Three authoritative source classes underpin the empirical analysis. Administrative damage determinations issued by MEUCC anchor the Damage Severity Index and permit spatial normalization by population; these records are the primary operative data. Copernicus Emergency Management Service rapid-mapping activation EMSR648 [10] and NASA ARIA displacement and damage-proxy products [11, 12] constitute the second source class, providing wall-to-wall spatial coverage for change detection and cross-checking against the administrative series. Complementary satellite-based approaches documented in the literature, including SAR and optical damage assessment pipelines [13, 14] and statistical characterization of the sequence [63], reinforce this validation chain. Agreement between the administrative and remote-sensing accounts is high in the four most affected provinces but diverges in peripheral areas where inspection lags extended beyond six weeks. In those cases, the remote-sensing layers are used to identify potential under-recording rather than to substitute for administrative data.

Practical reconciliation between administrative and remote-sensing sources proceeded on a layered cadence during the early post-disaster stages. Graded-damage rasters from Copernicus EMSR648 and ARIA coherence and displacement fields were overlaid on the provisional MEUCC tags at district and mahalle resolution, and cells in which the two accounts disagreed by more than approximately one severity class were flagged for follow-up rather than reconciled algorithmically. In the four most affected provinces, where field canvassing progressed in parallel with satellite acquisitions, subsequent inspection sweeps and appeal outcomes were adopted as the authoritative record, and the remote-sensing layers retained the role of independent verification rather than primary input. In peripheral areas where inspection lags extended beyond approximately six weeks, the remote-sensing layers were used prospectively to identify cells likely to be under-recorded in the administrative ledger, and these cells were marked for re-inspection at the next canvassing round rather than re-classified on the basis of the imagery. Reconciliation therefore operated as a validation chain in which the administrative record remained authoritative throughout but was audited continuously against wall-to-wall spatial coverage, with adjustments applied only through the statutory inspection process and not through post-hoc analytical substitution.

Turkish Statistical Institute (TÜİK) population registers [65] and the General Directorate of Mapping administrative boundaries supply the denominators and harmonized geographies required for consistent aggregation across provinces and time periods. Population denominators are taken from the 2022 address-based register, the most recent pre-event count available at provincial resolution. All diagnostic calculations use these denominators consistently, and sensitivity checks using 2021 and 2020 registers confirm that results are not sensitive to the choice of reference year within the plausible range. Night-time-light-based recovery monitoring, as recently demonstrated for the 2023 Türkiye–Syria event using SDGSAT-1 data [66], provides an additional independent lens for corroborating the province–month delivery trajectories reported in Section 3.

2.3. Damage Severity and Proportionality Diagnostics

Measured damage at provincial scale is summarized by a population-normalized index. The Damage Severity Index (DSI) expresses measured damage per resident, formed by adding the counts of collapsed, urgently demolishable and

heavily damaged buildings and dividing by the resident population; for readability, the numerator can be scaled per thousand without changing comparisons. For province i:

$$\mathrm{DSI}_i = \frac{C_i + U_i + H_i}{\mathrm{Pop}_i} \quad (1)$$

where, C_i, U_i, H_i denote administrative counts of collapsed, urgently demolishable and heavily damaged buildings, and Pop_i is resident population. Need shares are then defined as:

$$s_i^{\mathrm{need}} = \frac{\mathrm{DSI}_i}{\sum_j \mathrm{DSI}_j} \quad (2)$$

and allocation shares for aid or housing units are defined as:

$$s_i^{\mathrm{alloc}} = \frac{\mathrm{Alloc}_i}{\sum_j \mathrm{Alloc}_j} \quad (3)$$

Alignment between measured need and allocations is read in two complementary ways. First, a rank-based association checks whether provinces with higher damage also rank higher in allocations; second, a decomposable divergence gauges how far allocation shares depart from the shares implied by need, equalling zero when allocations are proportional to need and increasing as disproportionality grows. Monotonic association is conveyed by Spearman's rank correlation [67], which evaluates whether provinces with higher damage ranks also receive higher allocation ranks without assuming linearity or normality. In the no-ties case:

$$\rho_s = 1 - \frac{6\sum_{i=1}^{n} d_i^2}{n(n^2-1)} \quad (4)$$

with the standard tie-adjusted form used when ranks coincide [68]. Proportionality to need is summarized by the Theil T divergence from need shares to allocation shares [69]:

$$T = \sum_{i=1}^{n} s_i^{\mathrm{alloc}} \ln\left(\frac{s_i^{\mathrm{alloc}}}{s_i^{\mathrm{need}}}\right) \quad (5)$$

which equals zero under exact proportionality and increases as disproportionality grows [69, 70]. A Lorenz representation accompanies these summaries, plotting cumulative allocation against cumulative need ordered by ascending need share. Gini can be reported for completeness, but T is preferred for its decomposability and its direct proportional-to-need interpretation [70].

Uncertainty for both ρ_s and T is obtained via nonparametric bootstrap with resampling at the province level (1,000 replicates; percentile 95% intervals) [71, 72], and robustness is checked by 1% winsorization of extreme shares. These resampling and winsorization steps provide an internal verification that the alignment statistics are not driven by a small number of extreme provinces and that their qualitative ranking remains stable under modest perturbations of the data. Bootstrap inference is used here since, with only eleven provinces, closed-form large-sample approximations to the sampling distributions of ρ_s and T are not reliable, whereas resampling at the province level provides uncertainty estimates that respect the clustering structure without imposing strong distributional assumptions [72].

Population-based normalization is adopted in this study since the analysis concerns the distribution of housing and residential entitlements, for which resident counts provide the policy-relevant denominator. A qualification applies, nonetheless, to its interpretation. In provinces with relatively small resident populations but substantial non-residential infrastructure losses, such as damaged schools, hospitals, utility networks, or productive facilities, the DSI captures residential severity per capita and does not incorporate the functional or economic weight of infrastructure damage. Across the eleven affected provinces this effect is expected to be most relevant for smaller jurisdictions with dispersed rural settlement patterns, where the residential share of total physical loss is comparatively lower. The diagnostics reported here should therefore be read as instruments for monitoring housing allocation equity, and the findings for such provinces should be interpreted alongside separate indicators of infrastructure recovery where those are available. The alignment framework remains extensible through asset-based or value-weighted denominators for applications in which infrastructure equity is the primary object of analysis, and this extension does not alter the validity of the housing-oriented reading presented in this study.

2.4. Reconstruction Pace Index

The Reconstruction Pace Index (RPI) reports how quickly deliveries keep up with the rolling plan in each province and month. An RPI of one means delivery matches the plan for that month; values above one mean the plan was exceeded, and values below one indicates shortfalls. Reconstruction pace is measured at province–month resolution as a delivery-to-plan rate. For province i in month t:

$$\mathrm{RPI}_{it} = \frac{\mathrm{Delivered}_{it}}{\mathrm{Plan}_{it}} \quad (6)$$

In this specification, Delivered_{it} denotes the number of housing units officially handed over to entitlement holders in province i during month t, recorded at the point of administrative acceptance that closes the delivery cycle for each unit. Plan_{it} is the corresponding monthly target drawn from the rolling program schedule maintained by the lead delivery institutions and revised periodically to reflect site readiness, contractor mobilization, and updates in entitlement adjudication. The use of the rolling plan as denominator ensures that RPI_{it} reflects performance against the most recently committed schedule rather than the initial pre-event baseline; a pre-specified sensitivity analysis replaces the rolling denominator with the initial plan to test whether the substantive findings are sensitive to this choice.

Values may exceed one when deliveries outpace the plan; such exceedances are retained for analysis (rate interpretation) and, if needed, winsorized only for figures (capped at 2.0) while audit tables keep raw values. Observations with $\text{Plan}_{it} = 0$ and $\text{Delivered}_{it} > 0$ are flagged out-of-denominator and excluded from rate summaries but reported descriptively. Cases with $\text{Plan}_{it} = 0$ and $\text{Delivered}_{it} = 0$ are recorded as not applicable. These rules are pre-specified and applied uniformly to avoid induced zeros or artificial inflation of averages.

To detect persistent rather than transient shortfalls, an operational run rule is applied, which draws on standard statistical quality control practice in which a sequence of consecutive below-threshold observations signals a systemic deviation distinct from random variation [28]. A province–month is marked under-delivered when $\text{RPI}_{it} < 0.25$, and an early-warning condition is recorded when such under-delivery persists for two consecutive months; robustness considers thresholds in the interval [0.20, 0.33]. The run threshold is varied over this interval and the resulting provincial classifications are compared, confirming that the patterns discussed below are robust to reasonable changes in this tuning parameter.

The threshold interval of 0.20 to 0.33 is selected through a combination of operational reasoning and empirical stability. The lower bound of 0.20 corresponds to a monthly delivery rate at one-fifth of the rolling plan, a level at which shortfall cannot plausibly be attributed to within-month scheduling variation and indicates a substantive gap between capacity and plan. The upper bound of 0.33 corresponds to one-third of the rolling plan, beyond which classifying a province as under-delivering begins to absorb months that more plausibly reflect routine procurement cycles or seasonal construction slowdowns rather than sustained shortfalls. The central value of 0.25 preserves a conservative margin between these operational interpretations. The robustness check reported in Section 3.3 applies the run rule across this interval and identifies the same three provinces as triggering the early-warning condition at all three thresholds, confirming that the classification is stable within the pre-specified range. Extending the interval further in either direction would either lose substantive shortfalls below 0.20 or generate false positives above 0.33. The choice of threshold, while tuned to the administrative cadence of the Turkish reconstruction program, can in principle be recalibrated to the cadence conventions of other post-disaster settings.

When RPI_{it} is used in panel regressions, out-of-denominator months are removed from the dependent variable but remain in descriptive accounting; standard errors are clustered at the province level to account for serial correlation [73]. For distributional diagnostics (ρ_s, T), uncertainty is communicated by the province-level bootstrap described above.

All calculations are versioned and reproducible with open components. Administrative snapshots are time-stamped to handle subsequent revisions. Overlays between Copernicus polygons and ARIA coherence or displacement fields flag places where early building tags likely under or over-represent physical damage, and the alignment results are re-estimated under alternative masks to test sensitivity. To aid interpretation, Figure 6 maps alignment divergence and delivery pace onto a single response plane, with the highest values near zero divergence and pace equal to one. The surface summarizes an interpretive joint reading of the diagnostics: values peak when divergence approaches zero and pace is near one and decline as disproportionality increases or shortfalls persist. Axes denote DAA divergence on the x-axis, RPI on the y-axis, and a unitless quality index on the z-axis.

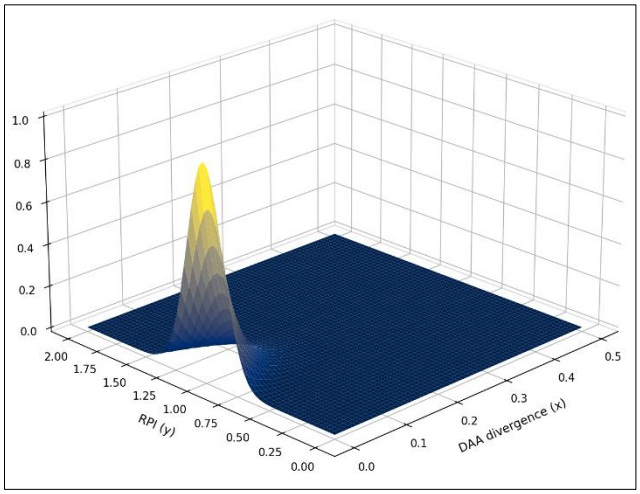

Figure 6. Recovery quality surface as a function of DAA divergence and RPI

Collectively, these design choices distinguish the diagnostics from more generic recovery indicators. DSI anchors need a population-normalized measure of severe building damage derived from administrative counts of collapsed, urgently demolishable, and heavily damaged buildings so that alignment is always read as allocations relative to measured damage per resident. DAA then combines Spearman's rank correlation [67], which checks whether provinces with higher damage also rank higher in allocations, with the Theil T divergence [69], which summarizes how far allocation shares deviate from the shares implied by need and equals zero under exact proportionality. RPI defines reconstruction pace as a province–month delivery-to-plan rate and applies pre-specified rules for months with zero denominators, exceedances, and a run threshold that highlights persistent rather than one-off shortfalls [28]. In combination, these elements move beyond simple completion ratios and aggregate aid totals by providing distribution-sensitive, rule-based diagnostics that can be implemented directly on existing administrative ledgers and associated monitoring products.

2.5. Compositional Analysis of the Damage Portfolio

Provincial severity is evaluated from the author-compiled corpus. For each province, counts of damaged dwellings, commercial premises, and barns are compiled; the province's share of the sample is reported; and the within-province composition across the three categories is summarized. Uncertainty for each share is conveyed by Wilson 95% confidence intervals, appropriate for proportions based on finite samples. All estimates are interpreted strictly on the sample frame; the values describe observations in the corpus rather than the entire population.

Let D_i, C_i, and B_i denote the numbers of observed damaged dwellings, commercial premises and barns in province i. The provincial sample total and its simplex share are:

$$S_i = D_i + C_i + B_i, s_i = \frac{S_i}{\sum_{j=1}^{n} S_j}, \sum_{i=1}^{n} s_i = 1 \tag{7}$$

with within-province composition:

$$p_{iD} = \frac{D_i}{S_i}, p_{iC} = \frac{C_i}{S_i}, p_{iB} = \frac{B_i}{S_i}, p_{iD} + p_{iC} + p_{iB} = 1 \tag{8}$$

Wilson 95% confidence intervals for each composition element, appropriate for proportions based on finite samples, are:

$$Wilson_{95\%} = \hat{p}_{ik} \pm \frac{z_{0.975}\sqrt{\frac{\hat{p}_{ik}(1-\hat{p}_{ik})}{S_i} + \frac{z_{0.975}^2}{4S_i^2}}}{1+\frac{z_{0.975}^2}{S_i}} \tag{9}$$

where, $z = z_{0.975} = 1.96$

Inter-provincial concentration is summarized on S_i through a Lorenz representation and the functionals [70]:

$$Gini = \frac{1}{\bar{S}n(n-1)} \sum_{i=1}^{n} \sum_{j=1}^{n} |S_i - S_j|, \; Theil_{unif} = \sum_{i=1}^{n} s_i \ln\left(\frac{s_i}{\frac{1}{n}}\right) \tag{10}$$

where, $n = 11$ is the province count and $\bar{S}$ is the mean of S_i. Bootstrap confidence bands for Gini and $Theil_{unif}$ are obtained by province-level resampling with re-normalization [71, 72].

To quantify how commercial observations rise with residential scale across provinces, a log–log model is fitted and the slope parameter β is reported with a normal-approximate 95 % confidence interval and R^2 on the log scale:

$$\log(C_i + 0.5) = \alpha + \beta \log(D_i + 0.5) + \varepsilon_i \tag{11}$$

A super-linear $\beta > 1$ is taken to indicate that commercial damage increases more than proportionally with residential observations. Pairwise differences between three-part composition vectors (p_i^D, p_i^C, p_i^B) are measured by the Jensen–Shannon divergence, with KL denoting the Kullback–Leibler divergence:

$$\mathrm{JS}(p, q) = \frac{1}{2} \mathrm{KL}\left(p \parallel \frac{p+q}{2}\right) + \frac{1}{2} \mathrm{KL}\left(q \parallel \frac{p+q}{2}\right) \tag{12}$$

For small S_i, Dirichlet–Laplace-smoothed shares are used to stabilise estimates:

$$\tilde{p}_{iD} = \frac{D_i+1}{S_i+3}, \tilde{p}_{iC} = \frac{C_i+1}{S_i+3}, \tilde{p}_{iB} = \frac{B_i+1}{S_i+3} \tag{13}$$

Nearest compositional analogues for each province are identified by selecting, for each row of the pairwise divergence matrix, the province with the smallest off-diagonal JS value. Results of this compositional analysis are reported as descriptive statistics in Section 3.1 and used to interpret the alignment and pace readings that follow.

2.6. Panel Econometric Strategy

Delivery performance is evaluated with a two-way fixed-effects panel. Let i index provinces and t months. The baseline specification is:

$$RPI_{it} = Z_{it}\beta + \alpha_i + \gamma_t + \varepsilon_{it} \quad (14)$$

where α_i and γ_t denote province and month fixed effects; standard errors are clustered at the province level to account for serial correlation and arbitrary within-province error dependence [73]. Here Z_{it} contains time-varying covariates and pre-specified phase interactions: the damage-severity decile is updated as post-event reassessments accrue, the accessibility index evolves as corridor and road restoration progresses, and the urbanization share is measured at the beginning of each panel year. Phase-by-covariate interactions are also included to allow the association between initial damage severity and delivery pace to differ between mobilization and production phases of reconstruction.

The design is descriptive: coefficients are interpreted as associations under fixed effects, not as causal effects [73, 74]. This choice reflects the circumstance that both allocations and reconstruction pace are the outcomes of non-random policy processes. Central and municipal decisions respond to unobserved factors such as political priority, lobbying capacity, pre-existing administrative capabilities, and local social capital, some of which evolve over time as well as across provinces, with the consequence that endogeneity concerns cannot be resolved by fixed effects alone. Possible reverse causality, for example, when central authorities adjust allocations in response to emerging delivery shortfalls, further complicates the attribution of causal direction. In the absence of credible instruments or sharp quasi-experimental variation in funding or eligibility rules, the panel estimates are therefore treated as structured descriptions of conditional associations rather than impact estimates.

In this setting, a two-way fixed-effects specification is preferred over random-effects or pooled models since the primary objective is to control for unobserved provincial heterogeneity and common temporal shocks while keeping identification explicitly descriptive in a policy environment where randomized allocation is neither expected nor ethically appropriate. The dependent variable is the province–month RPI, as defined in Section 2.4; the panel is estimated with province and month fixed effects and province-clustered standard errors. Covariates include pre-event damage severity, proxies for accessibility and logistics, and an urbanization share derived from official registers. Recent methodological cautions regarding two-way fixed-effects estimators are taken seriously [74]; alternative estimators are used as sensitivity checks when the identifying variation risks negative weighting or when adoption timing is staggered.

3. Results

The results are organized in four subsections. Section 3.1 reports sample-based severity diagnostics drawn from the author-compiled corpus, including Wilson 95% confidence intervals for commercial shares, commercial and agricultural intensity ratios relative to the residential denominator, Jensen–Shannon divergence between provincial composition vectors, and the log–log scaling between commercial and residential damage counts. Section 3.2 reports the Damage–Aid Alignment results for the eleven affected provinces, including the province-level allocation gap. Section 3.3 reports the Reconstruction Pace Index trajectories and the three provinces flagged by the run rule. Section 3.4 reports the two-way fixed-effects panel regression estimates.

3.1. Sample-Based Severity Diagnostics

Table 3 reports the within-sample commercial share for each province, together with Wilson 95% confidence intervals. The rank ordering indicates which provinces have a more urban-dominant damage profile versus those with more rural-exposed portfolios. Gaziantep leads with a commercial share of 37.1% (95% CI 34.4–39.9 pp), followed by Kahramanmaraş (29.1%, 27.4–30.8 pp), Hatay (28.1%, 26.9–29.3 pp), and Malatya (27.4%, 25.6–29.2 pp). At the other end of the distribution, Kilis (13.7 %, 5.8–21.6 pp) and Elazığ (17.1 %, 13.6–20.6 pp) show the lowest commercial shares and the widest intervals, reflecting both their smaller sample sizes and their more rural portfolio. Where one province's entire interval lies above another's, a reliably higher commercial share is indicated on this sample; where intervals overlap, differences should be treated as indistinguishable on the sample frame. As a corroborating check on the provincial structure captured by the corpus, the Spearman rank correlation between provincial shares in the corpus and provincial shares in the entitlement register reported in Section 3.5 is $\rho_s = 0.955$ ($p < 0.001$) across the eleven provinces, indicating that the corpus reproduces the inter-provincial distribution of severe damage that emerges from the official entitlement adjudication process.

Table 3. Commercial share by province with Wilson 95 % confidence intervals (percentage points)

Province	S_i	$p_{iC}(\%)$	95 % CI (pp)
Hatay	5,972	28.1	26.9 – 29.3
Kahramanmaraş	2,680	29.1	27.4 – 30.8
Malatya	2,459	27.4	25.6 – 29.2
Adıyaman	1,466	22.7	20.6 – 24.8
Gaziantep	1,191	37.1	34.4 – 39.9
Osmaniye	465	27.1	23.0 – 31.1
Elazığ	451	17.1	13.6 – 20.6
Diyarbakır	449	17.6	14.1 – 21.1
Şanlıurfa	397	25.4	21.1 – 29.7
Adana	325	18.5	14.3 – 22.7
Kilis	73	13.7	5.8 – 21.6

These composition readings feed directly into the diagnostic alignment reported in Section 3.2 and help interpret the pace results in Section 3.3, since urban-heavy portfolios tend to compress permitting and utility workloads, whereas rural-heavy portfolios stress distance-sensitive inspection and energization.

Table 4 reports, for each province, the compositional nearest neighbor identified by the smallest off-diagonal Jensen–Shannon divergence. Very small values in this table indicate near-identical mixes; this is observed most clearly for the Hatay–Kahramanmaraş pairing and for Elazığ–Kilis, which appear as mutual nearest neighbors with divergences close to zero. Several other provinces select close analogues within the same corridor: Malatya aligns most closely with Hatay; Osmaniye and Gaziantep align with Kahramanmaraş; and Adana aligns with Osmaniye. Not every match is symmetric: Adıyaman selects Şanlıurfa, whereas Şanlıurfa's nearest analogue is Malatya, a reminder that the neighbor relation is directed by the smallest divergence from each row.

Table 4. Compositional nearest neighbors by Jensen–Shannon divergence

Province	Nearest analogue	JS divergence
Hatay	Kahramanmaraş	0.00007
Kahramanmaraş	Hatay	0.00007
Malatya	Hatay	0.00028
Adıyaman	Şanlıurfa	0.00051
Şanlıurfa	Malatya	0.00031
Diyarbakır	Adıyaman	0.00207
Osmaniye	Kahramanmaraş	0.00201
Elazığ	Kilis	0.00111
Kilis	Elazığ	0.00111
Adana	Osmaniye	0.00537
Gaziantep	Kahramanmaraş	0.00569

The full pairwise divergence matrix is reported in Table 5. Diagonal zeros reflect identity, and the smallest off-diagonal entries in each row reproduce the nearest neighbors listed in Table 4. A loose cluster can be identified around Hatay, Kahramanmaraş, Malatya, Osmaniye and Gaziantep, where divergences remain at the lower end of the range, consistent with urban-dominant mixes. Larger values are observed for comparisons involving Şanlıurfa and Adana, indicating compositions that deviate more from the corridor average, typically more barn-weighted for Şanlıurfa and more commercial-weighted for Adana. Since the divergence is computed on the composition vector (p^D, p^c, p^B), the tables speak to mix similarity rather than absolute scale; provinces may therefore be compositionally close yet differ greatly in the total number of damaged assets. All values are multiplied by 10^3 for readability.

Table 5. Full Jensen–Shannon divergence matrix for provincial composition vectors (p^D, p^c, p^B)

Province\ Province	Hatay	K.maraş	Malatya	Adıyaman	Gaziantep	Diyarbakır	Osmaniye	Elazığ	Şanlıurfa	Adana	Kilis
Hatay	0	0.07	0.28	2.47	6.39	8.20	2.16	18.30	1.00	9.37	24.90
Kahramanmaraş	0.07	0	0.55	3.39	5.68	9.78	2.01	20.40	1.57	10.30	27.50
Malatya	0.28	0.55	0	1.53	6.10	6.96	3.78	14.60	0.31	10.50	20.90
Adıyaman	2.47	3.39	1.53	0	12.80	2.07	6.15	8.27	0.51	7.50	12.20
Gaziantep	6.39	5.68	6.10	12.80	0	25.00	13.00	28.60	8.32	30.80	39.70
Diyarbakır	8.20	9.78	6.96	2.07	25.00	0	10.80	6.89	4.61	5.52	7.80
Osmaniye	2.16	2.01	3.78	6.15	13.00	10.80	0	27.30	4.96	5.36	33.30
Elazığ	18.30	20.40	14.60	8.27	28.60	6.89	27.30	0	10.90	23.30	1.11
Şanlıurfa	1.00	1.57	0.31	0.51	8.32	4.61	4.96	10.90	0	9.58	16.30
Adana	9.37	10.30	10.50	7.50	30.80	5.52	5.36	23.30	9.58	0	24.50
Kilis	24.90	27.50	20.90	12.20	39.70	7.80	33.30	1.11	16.30	24.50	0

Table 6 normalizes composition using the residential denominator, so C_i/D_i reads the commercial intensity per damaged dwelling and B_i/D_i reads the agricultural (barn) intensity per damaged dwelling. Commercial intensity is highest in Gaziantep at roughly two-thirds of a commercial premise per dwelling, with Kahramanmaraş and Hatay following at a little over two-fifths; values in Malatya, Osmaniye, and Şanlıurfa cluster just below that range, and the lowest intensities are observed in Adana, Diyarbakır, and Kilis. The barn-to-dwelling ratio reveals a different pattern: Elazığ and Kilis stand out with the largest agricultural intensities, Gaziantep, Adıyaman, Şanlıurfa, and Diyarbakır form a mid-tier, and barn exposure is minimal in Osmaniye and Adana. These patterns are consistent with the composition results reported earlier: The Elazığ–Kilis pairing that emerged as compositionally closest on the JS metric is echoed here by similarly elevated B_i/D_i values, while the high C_i/D_i of Gaziantep and the moderate figures in Hatay and Kahramanmaraş align with the log–log scaling described below, where commercial counts rise faster than proportionally with dwellings.

Table 6. Commercial and agricultural intensity relative to the residential denominator

Province	(C_i/D_i)	(B_i/D_i)
Hatay	0.408	0.046
Kahramanmaraş	0.427	0.043
Malatya	0.399	0.058
Adıyaman	0.313	0.065
Gaziantep	0.639	0.084
Osmaniye	0.378	0.018
Elazığ	0.237	0.151
Diyarbakır	0.226	0.060
Şanlıurfa	0.363	0.065
Adana	0.230	0.015
Kilis	0.182	0.145

Operationally, provinces toward the top of the commercial ratio are expected to face denser permitting and utility re-energization in business districts, whereas provinces with high barn intensity will require distance-sensitive inspection and agricultural support in parallel with housing programs. These normalized intensities serve as interpretable inputs for the alignment reading in Section 3.2 and as priors for reading pace in Section 3.3, since the mix of commercial and agricultural workloads conditions how quickly reconstruction can be executed.

Figure 7 displays the log–log scale relation between observed commercial and residential damage counts across the eleven provinces, together with the ordinary least-squares fit and a 95 % mean confidence band. The slope estimate is $\beta = 1.20$ (95 % CI $[1.02, 1.37], R^2 = 0.965$), confirming a super-linear scaling: commercial damage rises more than proportionally with residential observations, and the lower bound of the confidence interval remains above unity at the 95 % level. The fit is close across the corridor but shows modest leverage from Gaziantep, whose high commercial intensity contributes to pulling the slope above one. This scaling is consistent with concentrated commercial exposure in urban cores where residential losses are also large, and it explains why provinces compositionally closest to Hatay and Kahramanmaraş tend to carry the densest permitting and utility workloads. The log(·+0.5) transformation stabilizes the fit for provinces with small absolute counts without altering the qualitative ordering of the scatter.

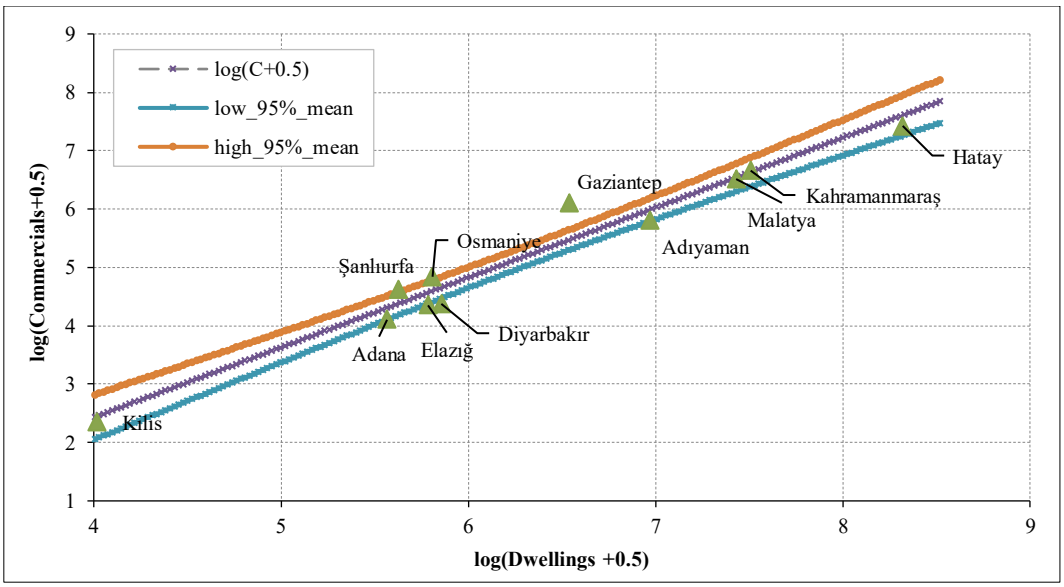

Figure 7. Scale–mix relation on the log–log plane with ordinary least squares fit and 95% mean confidence band

Collectively, the compositional analysis clarifies that similar overall damage totals can conceal very different mixes of dwellings, commercial premises, and barns and that these mixes condition the administrative and utility workloads municipalities face during reconstruction. Provinces that are compositionally close can be expected to face similar inspection sequencing, permitting loads, and re-energization tasks, which justifies borrowing implementation playbooks while adjusting only for scale. Provinces that are compositionally distinct should be treated as requiring tailored mixes of housing, workplace, and rural-livelihood interventions. This information links back to the diagnostics that follow: compositionally similar provinces are expected to produce comparable need shares in the alignment measure, and their reconstruction pace can be interpreted against analogous portfolios where permitting, inspection, and utility constraints are of similar character.

3.2. Damage–Aid Alignment

Alignment between population-normalized damage and housing entitlement allocations is summarized in Table 7. Across the eleven provinces, Spearman's rank correlation between need shares and allocation shares is $\rho_s = 0.836$ ($p = 0.001$, 95% bootstrap CI [0.402, 0.991]) [67, 71], indicating a strong positive association. Provinces with higher population-normalized damage generally received larger allocation shares. The Theil T divergence is 0.087 (95% CI [0.031, 0.174]) [69], confirming that while the rank ordering is broadly consistent with need, allocation shares depart meaningfully from proportionality. Both statistics are stable under 1% winsorization of extreme shares ($\rho_s = 0.836$, $T = 0.081$), confirming that the results are not driven by outlying provinces.

Table 7. Damage–Aid Alignment by province

Province	DSI	Need %	Allocation %	Δ (pp)	Assessment
Hatay	3.543	24.6	35.0	+10.4	Over-allocated
Malatya	3.028	21.0	17.9	−3.1	Under-allocated
Kahramanmaraş	2.281	15.8	17.9	+2.1	Close to need
Adıyaman	2.312	16.1	10.1	−6.0	Under-allocated
Osmaniye	0.830	5.8	2.9	−2.9	Under-allocated
Elazığ	0.764	5.3	3.4	−1.9	Under-allocated
Kilis	0.503	3.5	0.4	−3.1	Under-allocated
Gaziantep	0.559	3.9	4.5	+0.6	Close to need
Diyarbakır	0.249	1.7	3.7	+2.0	Slight over
Şanlıurfa	0.180	1.3	2.5	+1.2	Close to need
Adana	0.143	1.0	1.8	+0.8	Close to need

The provincial pattern in Table 7 reveals interpretable heterogeneity. Hatay receives an allocation share of 35.0%, compared with a need share of 24.6%, a departure of 10.4 percentage points. As the province with both the highest absolute damage count and the most complex reconstruction portfolio, including heritage precincts, coastal terrain, and a displaced population in the hundreds of thousands, this concentration is consistent with proportional programming requirements and the scale of the logistical task, though the departure from need proportionality remains large.

Adıyaman presents the sharpest under-allocation relative to need: a need share of 16.1% against an allocation share of 10.1% (6.0 pp below need). Malatya and Kilis each show moderate underrepresentation of 3.1 pp. Kahramanmaraş, Diyarbakır, Şanlıurfa and Adana remain approximately within ±2 pp of their need shares and are classified as close to need.

Figure 8 presents a Lorenz curve of cumulative allocation against cumulative need, ordered by ascending need share. The curve lies below the 45° line for low-need provinces and above it for the highest-need group, consistent with moderate concentration around Hatay. The Theil T value of 0.087 falls in the lower range of divergences reported for post-disaster resource allocation studies, suggesting that while the program is broadly proportional to need, scope remains for adjustments in favor of Adıyaman and Kilis in subsequent programming cycles. The bootstrap percentile intervals for T ([0.031, 0.174]) exclude zero, confirming that the observed departures from strict proportionality are statistically distinguishable from sampling variation [71, 72].

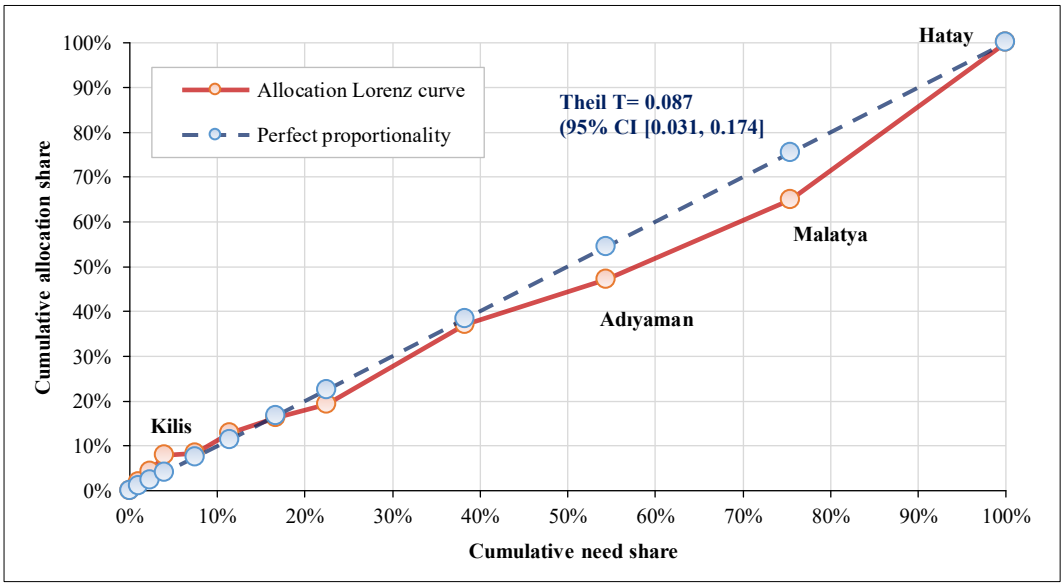

Figure 8. Lorenz curve of cumulative entitlement allocation share against cumulative need share; provinces ordered by ascending DSI

3.3. Reconstruction Pace Index

Provincial Reconstruction Pace Index trajectories over the eighteen-month observation window (March 2023 through August 2024) are summarized in Table 8. Mean RPI across all valid province–month observations range from 0.446 (Kilis) to 1.050 (Gaziantep), with a standard deviation of 0.218 across provincial means. Three provinces record mean values at or above the rolling plan threshold of 1.0 — Gaziantep (1.050), Adana (1.030) and Osmaniye (1.004), indicating that deliveries matched or exceeded the rolling plan over the observation period. Two additional provinces, Kahramanmaraş (0.969) and Şanlıurfa (0.939), remained just below the plan with mean shortfalls of less than seven percentage points, consistent with stable, near-plan delivery rather than systemic under-performance. Three provinces trigger the run rule [28] under the baseline threshold of 0.25 for two or more consecutive months: Adıyaman (August 2023), Elazığ (September and October 2023) and Kilis (August 2023).

Table 8. Reconstruction Pace Index by province (March 2023 – August 2024)

Province	Mean RPI	Min RPI	N (obs)	Run rule	Warning months
Gaziantep	1.050	0.045	15	No	—
Osmaniye	1.004	0.048	14	No	—
Adana	1.030	0.047	15	No	—
Kahramanmaraş	0.969	0.049	14	No	—
Şanlıurfa	0.939	0.052	14	No	—
Diyarbakır	0.872	0.050	14	No	—
Malatya	0.840	0.051	13	No	—
Hatay	0.774	0.051	13	No	—
Adıyaman	0.604	0.051	13	Yes	Aug 2023
Elazığ	0.462	0.050	12	Yes	Sep–Oct 2023
Kilis	0.446	0.051	13	Yes	Aug 2023

The early-warning condition in Adıyaman is attributable primarily to contractor mobilization delays at one of the primary public-delivery sites in the province, where rocky terrain required extended foundation preparation. Elazığ records the longest mobilization period of the eleven provinces, with three months between plan activation and first meaningful delivery, consistent with its high agricultural intensity and the dispersion of eligible sites across rural areas where access road preparation preceded construction. Kilis, the smallest province by entitlement volume, exhibits the highest relative variance in monthly delivery, reflecting the sensitivity of small-contract programs to procurement timing. In all three cases the run-warning condition clears within two months of onset, and monthly RPI values converge toward or above the corridor average by the fourth quarter of 2023.

The robustness checks across thresholds of 0.20, 0.25, and 0.33 identify the same three provinces under all specifications, confirming that the pattern is not sensitive to the choice of run-rule threshold within the pre-specified interval [0.20, 0.33] [28]. Hatay records the lowest mean RPI among the four highest-damage provinces (0.774), a figure consistent with the scale and complexity of its reconstruction portfolio rather than administrative under-performance. Malatya (0.840) follows, which reflects a period of plan revision associated with replanning of dense residential zones. Notably, no province triggers the run rule after the fourth quarter of 2023, indicating that the flagged shortfalls reflect mobilization-phase frictions rather than sustained systemic under-delivery.

3.4. Panel Regression

Two-way fixed-effects panel regression results are reported in Table 9. The pre-event damage severity decile carries a negative and statistically significant coefficient ($\beta = -0.041$, SE = 0.016, $p = 0.013$), indicating that provinces in higher damage deciles deliver at a lower pace relative to their own rolling plans, conditional on province and month fixed effects. This association is consistent with the operational interpretation that severe damage generates a more complex reconstruction task, with denser debris, more extensive infrastructure preparation, and larger permitting workloads that delay delivery even when resources are proportionally committed.

Table 9. Two-way fixed-effects panel regression results

Covariate	β	SE	p-value	Interpretation
DamageDecile	−0.041	0.016	0.013	Higher damage → slower pace
UrbanShare	+0.033	0.013	0.017	Urban profile → faster delivery
Access	+0.026	0.011	0.022	Accessibility → faster delivery
Phase2 × Damage	+0.052	0.020	0.012	Damage gap narrows in later phase

Urban share and site accessibility both carry positive and statistically significant coefficients ($\beta = +0.033$ and +0.026, respectively), consistent with the expectation that urban portfolios compress permitting and utility re-energization cycles, whereas accessible sites reduce travel time for inspection and materials delivery. The Phase 2 interaction with damage severity ($\beta = +0.052$, $p = 0.012$) indicates that the negative association between damage severity and pace attenuates in the later phase of the panel, consistent with the interpretation that high-damage provinces close the delivery gap as mobilization completes and production scales. Within-province R^2 is 0.59, indicating that the covariates explain a substantial share of province-level variation in monthly pace beyond what is captured by province and month fixed effects.

All coefficients are interpreted as conditional associations rather than causal effects [73, 74]. Both allocations and reconstruction pace reflect non-random policy decisions that respond to unobserved provincial characteristics, and the panel design cannot rule out reverse causality between delivery pace and subsequent allocation adjustments. The results are nonetheless informative as structured descriptions of the conditional relationships between provincial characteristics and delivery performance, and they are consistent with the governance interpretation developed in Section 1.2 and elaborated in the Discussion.

3.5. Reconstruction Entitlements

Entitlement adjudication figures published in the TERRA report [15] as of mid-January 2024 provide the legal baseline against which the pace diagnostics of Sections 3.3 and 3.4 are read. As of that date, approximately 439,622 entitlements had been accepted across the eleven provinces: 387,776 for dwellings, 40,422 for businesses, and 11,424 for barns. Table 10 reports the full provincial distribution. Concentration is marked in Hatay (151,984), followed by Malatya (80,104), Kahramanmaraş (78,584), and Adıyaman (45,461), with a long tail across Gaziantep (19,922), Diyarbakır (15,806), Elazığ (15,248), Osmaniye (12,653), Şanlıurfa (10,891), Adana (7,224), and Kilis (1,745). These stocks constitute the denominator for program mix inspection workloads and utility staging that condition the pace trajectories reported earlier.

Table 10. Provincial entitlements by asset class as of January 2024

Province	Housing units	Commercials	Barns	Total
Hatay	135,603	15,603	778	151,984
Malatya	69,397	8,121	2,586	80,104
Kahramanmaraş	69,228	7,642	1,714	78,584
Adıyaman	39,094	3,397	2,970	45,461
Gaziantep	17,421	1,662	839	19,922
Diyarbakır	14,232	991	583	15,806
Elazığ	13,343	703	1,202	15,248
Osmaniye	11,236	1,296	121	12,653
Şanlıurfa	9,799	651	441	10,891
Adana	6,864	318	42	7,224
Kilis	1,559	38	148	1,745
Total	**387,776**	**40,422**	**11,424**	**439,622**

The urban–rural composition of entitlement stocks is reported in Table 11. Of the 387,776 total dwelling entitlements, 282,895 are urban and 104,881 rural. On-site transformation joint applications under the Yerinde Dönüşüm program total 102,466 urban and 23,028 rural, whereas near-term lottery draws cover 207,586 beneficiaries and 45,321 housing units. The provincial signatures are highly asymmetric: Hatay records 117,731 urban beneficiaries and the single largest near-term draw, whereas Kahramanmaraş and Adıyaman carry substantial rural shares and disproportionately high volumes of on-site applications.

Table 11. Provincial entitlements and near-term delivery staging [15]

Province	Beneficiaries - Urban	Beneficiaries – Rural	On-site Applications - Urban	On-site Applications - Rural	Lottery Beneficiaries	Lottery Dwellings
Adana	5,610	1,254	1,881	331	1,855	1,589
Adıyaman	23,387	15,707	8,050	2,731	17,064	2,218
Diyarbakır	10,830	3,402	2,710	994	8,711	1,423
Elazığ	9,006	4,337	1,044	628	6,201	2,255
Gaziantep	10,515	6,906	3,041	2,172	9,587	10,698
Hatay	117,731	17,872	49,891	4,115	81,006	7,275
Kahramanmaraş	44,177	25,051	16,636	7,109	27,635	9,289
Kilis	435	1,124	149	300	1,884	1,103
Malatya	48,529	20,868	12,596	2,872	42,574	6,181
Osmaniye	7,766	3,470	4,253	812	8,795	1,976
Şanlıurfa	4,909	4,890	2,215	964	2,274	1,314
Total	**282,895**	**104,881**	**102,466**	**23,028**	**207,586**	**45,321**

4. Discussion

The diagnostic findings presented in the preceding section acquire their full interpretive weight when read against the operational chain that produced them. Each is shaped by a sequence that begins with the speed and quality of damage signals in the first fortnight, passes through the siting and servicing of transitional settlements, and culminates in the legally sequenced conversion of entitlements into handed-over housing units.

4.1. Rapid Damage Assessment and Operational Decision-Making

Rapid assessment in the first weeks operated as a layered system, with administrative inspections, satellite-derived proxies and field intelligence arriving on different cadences and at different spatial resolutions. Outputs followed a layered cadence: administrative tags rolled near-continuously, graded-damage rasters updated with satellite passes [10, 11], and coherence fields flagged corridor-scale anomalies [12, 14], together producing denominators suitable for sub-district analysis.

Administrative inspections undertaken by the Ministry of Environment, Urbanization, and Climate Change (MEUCC) generated the earliest building-level determinations and opened a resident-facing channel through the Damage Assessment Inquiry service. As neighborhoods were canvassed and appeals worked through the queue, these determinations evolved from indicative tallies into a working baseline for local severity. Humanitarian partners mirrored the ministry record by aggregating building classifications to the mahalle level as collapsed, urgently demolishable, and heavily damaged [61], thereby producing the first comprehensive denominators suitable for spatial analysis below the district scale.

Earth-observation layers supplied wall-to-wall coverage where inspections could not keep pace and offered independent checks once field access improved [13, 62, 64]. These spatial products were interpreted in light of geophysical reconstructions of the doublet's kinematics, including multi-segment rupture and possible intervals of high rupture velocity [4–9], which help explain the heterogeneous footprint of severe shaking across provincial capitals and intermediate-density corridors. Standard practice links signal production to decision cells with defined mandates, routing quality-controlled tags, graded-damage editions, and coherence alerts to teams empowered to act at the appropriate spatial and legal scales. The damage and needs assessment approaches used by development partners emphasize population-normalized indicators, traceable uncertainty, and clear separation of measured destruction from modeled impacts when triaging scarce resources in the first weeks [15]. Within Türkiye's legal architecture, as introduced in Section 1, TAMP [29] channeled these technical inputs through sectoral service groups at national, provincial, and municipal levels, linking signal production to decision cells with defined mandates.

4.1.1. From Signals to Decisions

Operational decisions in the first fortnight were steered as much by the availability of verifiable signals as by the absolute magnitude of local need. AFAD's public briefings document the rapid escalation to a level four national emergency, the pace of international assistance acceptance, and the cadence of urban search-and-rescue deployment as windows of survivability closed [1]. Those briefings also record the handover from life-saving operations to recovery functions as the focus shifted toward stabilization and service restoration. The international interface was unprecedented in scale. The INSARAG after-action review [75] describes the largest international USAR mobilization in the network's history, documenting the deployment of 199 international rescue teams, 49 of them INSARAG-classified, comprising roughly 11,000 search-and-rescue personnel, and noting where geospatial products and local tasking information converged to optimize team placement and highlighting the operational benefits of shared situational awareness under surge conditions.

Lifeline restoration drew on the same hybrid of administrative tallies, satellite products, and field reports. Copernicus graded damage maps [10] and ARIA coherence anomalies [11, 12] were used to visualize blocked corridors and districts with concentrated destruction, informing debris-clearance priorities and routing for fuel, water, and medical logistics when terrestrial communications were intermittent. Municipal utilities and provincial coordination cells integrated these layers with crew reports to sequence repairs to substations, trunk mains, and health facilities, a process that became progressively more data-driven as additional satellite passes and manual vetting improved coverage and confidence.

Shelter siting decisions brought data and constraints into even sharper relief. Administrative tags indicated where housing destruction was concentrated; remote-sensing outputs corroborated those patterns and flagged peripheral settlements with access constraints; and municipal land banks, rights-of-way and proximity to services narrowed feasible sites for large-footprint tent and container settlements. OCHA situation reporting from mid-March through late March captured the transition from dispersed displacement to the consolidation of formal and informal sites [76], with International Organization for Migration estimates of roughly three million people displaced in the early months and more than two million residing in temporary settlements as arrangements stabilized. In practice, siting choices reflected a balance between rapid occupancy, connection to potable water and power, and transport access for supply chains, with provincial differences in available public land and pre-existing infrastructure shaping outcomes.

Figure 9 traces the policy pathway from post-earthquake damage tags to financing and siting decisions, with quality gates at permitting and inspection so delivery is assessed in legal as well as engineering terms. Owner-rebuild and government-rebuild pathways populate the RPI denominator differently, since rolling municipal plans and program contracts carry different temporal structures, while repair and retrofit cases enter the alignment read through per-capita loan and grant allocations rather than new-unit counts.

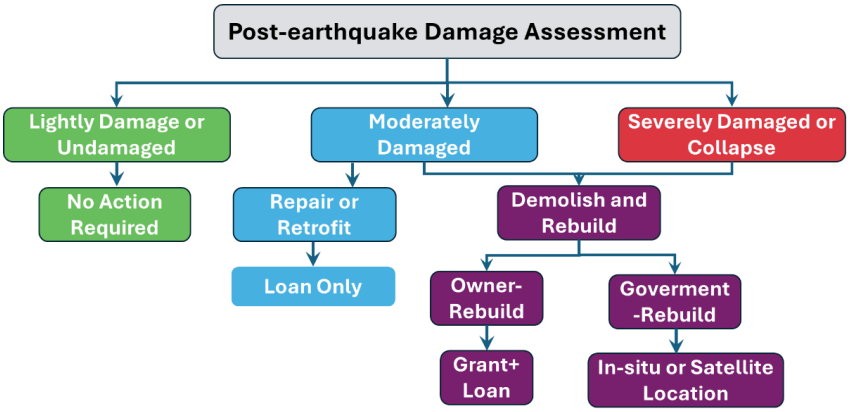

Figure 9. Policy pathway from post-earthquake damage tags to financing and siting decisions

4.1.2. Interoperability, Latency, and the Last Mile

The same record makes visible the points at which assessment signals did not convert to action at the required pace. Communications failures and winter weather limited the flow of verified information from district municipalities to provincial and national coordination cells, and delays in reconciling conflicting inputs generated pockets of under-supply in some districts and duplication in others. The INSARAG review identifies several technical and procedural lessons from this interface, pre-agreed data standards for tasking, simplified common operating pictures that can be used by mixed-capability teams, and clearer protocols for how geospatial products should be prioritized against ground reports when time windows are short. OCHA's contemporaneous situation reports, read together with municipal debriefs, show how staff in local governments and volunteer networks improvized ad hoc channels, often including low-bandwidth messaging, public mapping portals, and radio, to overcome gaps in official communications when hierarchies lagged [76]. Research groups documented parallel experiments in crowdsourcing distress signals and needs through social media classification. Although such tools offered situational awareness under bandwidth constraints, their integration into formal tasking was uneven without validation pipelines and duty-of-care protocols [77].

Interoperability challenges were not only technical. They were institutional questions about how swiftly municipal mandates could be exercised within the national framework set by TAMP [29], how rapidly provincial and district units could certify sites and permits for emergency settlements, and how inspection and utilities could be surged to match the spatial pattern of need. Where delegation and rehearsed procedures were clear, assessment signals flowed more quickly into team tasking, lifeline repair, and settlement siting. Where they were not, satellite maps and administrative tallies accumulated without commensurate operational traction, and corrective effort was required to close the loop between information and action.

Two implications follow for the evaluation reported in Section 3. First, the moderate but non-negligible Theil T divergence of 0.087 is a joint product of measurement and the institutional pathways that carry it to the field; reading the alignment ratio without attention to governance can misdiagnose operational frictions as inequity or vice versa. Second, the three provinces flagged by the RPI run rule (Adıyaman, Elazığ, and Kilis) are provinces where, at the moment the warning triggered, early information architecture and procedural readiness lagged behind the scale of local need; provinces where damage signals were consolidated sooner and where municipal processes for siting, permitting, and inspection were able to scale were better positioned to sustain delivery trajectories months later.

4.2. Temporary and Transitional Settlements

The first weeks were defined by velocity and scale. Approximately 350 tent compounds were established across the corridor, and close to one million tents were moved into the affected provinces [15, 61]. As camp management matured, prefabricated modules closed the gap between emergency tenting and durable plots and shortened the period in which families had to choose between proximity to work and access to schooling or care.

The container network then formed the backbone of daily life during the transitional phase. By the first anniversary, 392 container settlements were operating, with about 211,000 containers hosting approximately 675,300 residents [15]. Figure 10 integrates the allocation of installed containers across provinces for urban compounds and rural sites together with the sheltered population by setting them. The urban stock is concentrated in Hatay, Malatya, Adıyaman, and Kahramanmaraş, with Gaziantep and Osmaniye forming a minor tail. The rural stock is led by Kahramanmaraş and Adıyaman, followed by Hatay, Gaziantep, Malatya, and Osmaniye. Translated into persons sheltered, the signatures are distinct: Hatay is primarily urban, Malatya is urban-dominant, Adıyaman is mixed with a rural tilt, Kahramanmaraş is balanced, Gaziantep is rural-leaning at a lower scale, and Osmaniye is small.

Two policy inferences follow. First, urban-dominant provinces concentrate demand on permitting, inspection, and utility re-energization since dense compounds generate routine service loads. Pace is therefore conditioned by these gates, which is consistent with the positive UrbanShare coefficient observed in the panel regression. Second, rural-tilted provinces face distance-aware logistics as dispersed sites protect land-anchored livelihoods while stretching supervisory and utility runs. Pace is governed by travel time and synchronized restoration of water and power, which is consistent with the positive access coefficient and with the observation that Elazığ, Kilis, and parts of Adıyaman, provinces with the highest barn-to-dwelling ratios in Table 6, were among those flagged by the run rule in Table 8. Alignment should thus be read not only as volume proportionality but also as the appropriateness of instrument choice to the spatial pattern of settlement.

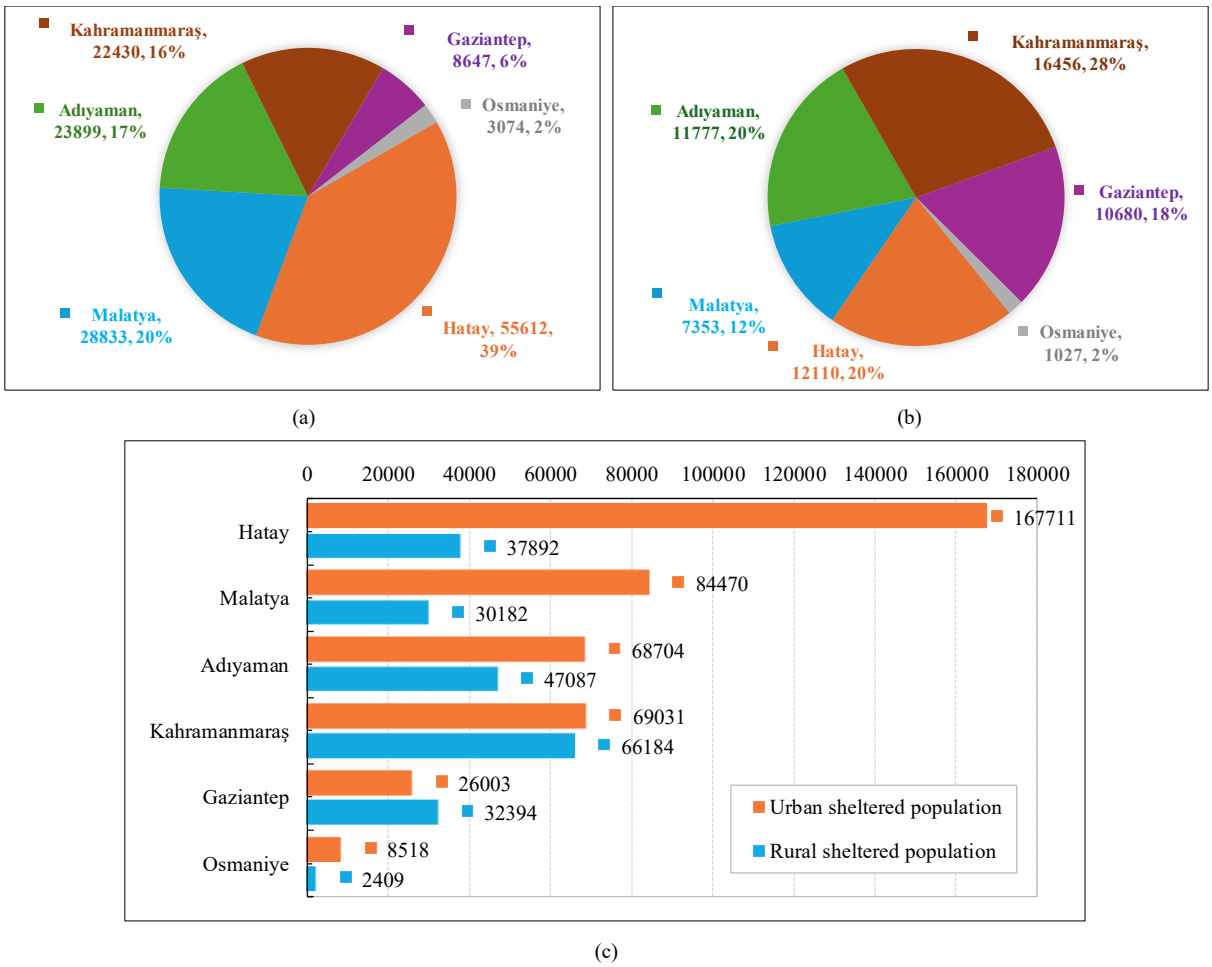

Figure 10. Container settlements across the six most affected provinces: (a) installed containers in urban compounds; (b) installed containers in rural sites; (c) sheltered population by setting

At site scale, Figure 11 sets out a governable anatomy. Hard-standing surfaces and an orthogonal plot grid establish numbered, inspectable bays and fire breaks; circulation lanes sized for emergency and service vehicles enable predictable routing for waste, water, and fuel. Paved pedestrian corridors with modular service units create activity spines for complaints, payments, and basic care. Regularly spaced utility spines reduce walking distances, simplify supervision, and support lighting that improves perceived safety. On sloped sites, terraced benches adapt the layout to topography, preventing runoff and mud whilst preserving sightlines for security and inspection. Where compounds adjoin existing districts, proximity to bus routes, schools, and health posts shortens trips and reconnects households to ordinary urban rhythms.

Figure 11. Representative container-settlement layouts in Gaziantep and Kahramanmaraş [15]

The spatial distribution was intentionally mixed. Large urban compounds were complemented by rural sites so that smallholders and peri-urban households could preserve land-anchored livelihoods while essential services were restored. Provincial figures show a pronounced concentration in Hatay, Kahramanmaraş, Adıyaman, and Malatya, whereas the remaining provinces sustained smaller, yet operationally significant, sites integrated into municipal service grids. The practical consequence was prosaic but decisive: a container address allowed utility connections, opened a service account, and gave grievance systems and social services a stable place to operate without improvization each morning.

Shelter retained a humane character since it traveled with cash and utilities. Camp card instruments circulated inside the settlements; monthly rent support reached both owners and tenants; and food security was stabilized by mobile kitchens and bakeries sized to predictable daily volumes. Transfers did not lose weight, but they changed the texture of waiting: households could purchase what they needed rather than queue for whatever arrived, pressure to remain in tents eased when safer alternatives existed, and queue management lightened as choice returned. In the ordinary language of cities, these devices mark the difference between a queue and the outline of a community. The urban–rural compound distribution documented in this section also helps interpret the positive UrbanShare coefficient (+0.033) in Table 9. Provinces whose shelter geographies were concentrated in dense compounds generated the kind of repeatable permitting and utility loads that municipal gates process routinely, whereas dispersed rural siting stretched supervisory runs in ways consistent with the positive Access coefficient (+0.026).

4.3. Reconstruction Programming and Entitlements

Reconstruction began as a legal and administrative promise. Entitlement adjudication converted damage assessments and appeals into a right that could be exercised either as a public allocation or as support for on-site rebuilding. The complete provincial distribution of adjudicated entitlements is reported in Table 10, with aggregate totals of 387,776 dwellings, 40,422 businesses, and 11,424 barns [15]. Read operationally, the entitlement stocks in Table 10 constitute the denominator for program mix, inspection workloads, and utility staging. Dwelling-heavy urban portfolios imply network-centric constraints, whereas provinces with sizable barn and rural components require distance-aware logistics and rural-livelihood supports, including service extensions to sheds and storage, all-weather access, and on-farm siting and inspection. The pace of reconstruction and the alignment between measured damage and allocations should therefore be interpreted against this legal baseline.

The concentration pattern (largest in Hatay, followed by Malatya, Kahramanmaraş, and Adıyaman) accounts for the divergence in permitting and inspection workloads that followed, and the urban–rural split conditions the mix of plan revisions and single-parcel actions that municipalities needed to process. The urban–rural composition of entitlement stocks is displayed in Figure 12. Housing is urban-dominant in Hatay and Malatya; Kahramanmaraş and Adıyaman exhibit substantial rural shares; workplaces are concentrated in urban corridors across all provinces; and barn entitlements are overwhelmingly rural, with notable concentrations in Adıyaman, Kahramanmaraş, Malatya, and Elazığ. Urban-dominant portfolios imply network-centric constraints since dense compounds and business corridors create concentrated, routine service demand. Rural-tilted portfolios imply distance-aware logistics as households remain close to fields, sheds, and small workshops.

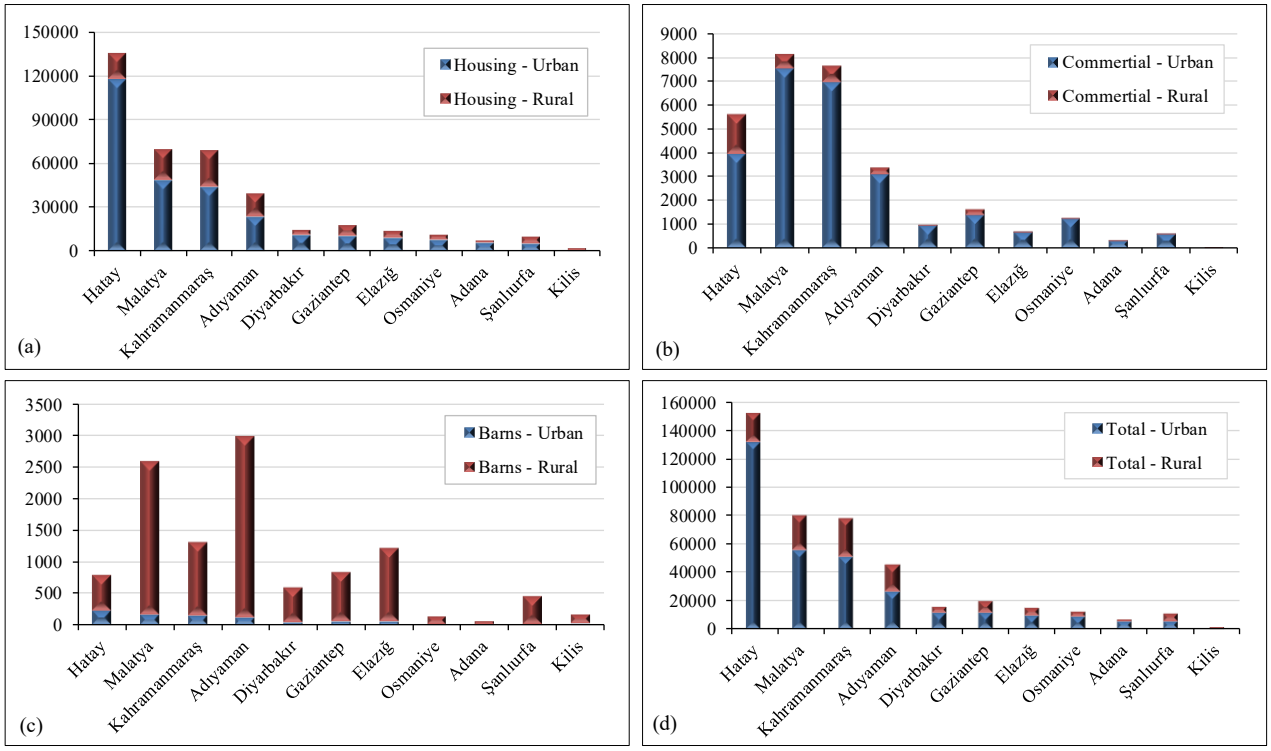

Figure 12. Urban–rural distribution of entitlements by province: (a) housing; (b) workplaces; (c) barns; (d) total

Drawing on the urban–rural staging reported in Table 11, the geography of delivery is highly asymmetric. Hatay exhibits a pronounced urban profile and the largest near-term draw, implying network-centric constraints as keys are released. Malatya is likewise urban-dominant with a substantial draw. By contrast, Kahramanmaraş and Adıyaman carry significant rural shares and high volumes of on-site applications, signaling distance-aware logistics for permitting, inspection, and temporary service extensions around farms and sheds. Mid-scale portfolios in Gaziantep, Diyarbakır, and Elazığ suggest mixed strategies: corridor-based public delivery in town paired with targeted on-site rebuilds outside.

Two instruments then operated side by side. Public delivery under TOKİ, Emlak GYO and the ministry's directorates advanced where replanning, infrastructure, and density targets demanded a site-wide approach; on-site rebuilds under Yerinde Dönüşüm combined grant and zero-interest credit for entitled owners whose parcels satisfied geotechnical and planning requirements. The duality was not administrative duplication: in dense cores and heritage precincts, parcel geometry, rights-of-way, and the need for accessible open space made site-wide replanning the only credible way to achieve safety without years of ad hoc exceptions; in rural belts and small towns where household economies are tied to fields and sheds, on-site rebuilding preserved livelihoods at a public cost the system could carry. What unified the portfolio was not a single architectural language but a common chain of legality: revised plans, permits, inspection logs, material certificates, and as-built files. Inspection capacity had to rise with production rather than chase it; any lag would accumulate as a quiet deficit that surfaces only after keys are handed over.

Entitlement numbers determine cadence and sequence. They set the order for utility extensions, the volume of social infrastructure needed to prevent dormitory districts, and the rhythm of public draws that anchors expectations to a calendar. Integration among damage-assessment software, the national address base, insurance records, and ministerial databases shortens the path from a field tag to an entitlement executable in law and finance. Although largely invisible to residents, these couplings explain predictable announcements and the avoidance of exception-heavy contracting, and they translate directly into the RPI denominator whose behavior was reported in Table 8.

4.4. Resettlement and Social Protection

For many households, permanence was preceded by safety and routine. Movement typically ran from a damaged neighborhood to a tent street and then to a container grid; schooling resumed in prefabricated classrooms, clinical care in modular wards, and decisions on permanent siting and finance followed confirmation of entitlement status and parcel conditions. Social protection functioned as connective tissue: regular and temporary programs expanded, provincial funds moved substantial cash volumes, and psychosocial and child-protection teams operated alongside logistics. DNA-assisted reunification, kinship care, day-care access for bereaved children and targeted transfers for older adults and people with disabilities appear as administrative rows but are experienced as the ability to plan a day not consumed by contingency [78, 79].

Transitional social infrastructure is illustrated in Figure 13, which shows a modular school courtyard on hard standing, where an orthogonal plot grid and open sightlines enable safe assembly and inspection; reduce dust and mud; shorten walk distances for younger pupils; and allow emergency access without obstruction; a traffic-calmed corridor where children can move independently between living units and services, with continuous surfaces, edge seating, and clear wayfinding lowering the daily effort of reaching water points, classrooms, and care [78]; and a psychosocial and social-assistance unit with bench seating and posted information, signaling predictable hours and accessible grievance and support channels [79]. Together, these elements convert container stock from temporary storage into habitable urban fabric governed by simple, inspectable rules; residents experience the change as the return of routine.

(a) (b) (c)

Figure 13. Transitional social infrastructure in container settlements: (a) modular school courtyard on hard-standing with open sightlines; (b) traffic-calmed residential corridor enabling safe movement for children; (c) psychosocial and social-assistance unit with seating and posted information [78, 79].

Hosting outside the zone complemented camps and containers. Programs that matched evacuees with host families were numerically smaller than formal settlements, yet they mattered since they reduced the serviced-plot denominator

and preserved social ties at a moment when networks were fragile. These choices later became visible in school class sizes, clinic lists and municipal service billing. The arc is easy to describe and difficult to deliver: households began to make decisions in an environment where cash instruments were predictable, services were close enough to stitch routines back together, and complaint lines answered within the times that had been promised when tents were still being erected.

The fragility of networks described above and the stabilizing effect of predictable cash and services underpin one reason why provinces with the fastest recovery of daily routines (Gaziantep, Adana, and Osmaniye) also appear at the top of the pace distribution in Table 8, whereas provinces where transitional social infrastructure took longer to scale cluster toward the bottom of the same ranking.

4.5. Reconstruction in Practice

Land-use decisions governed the trade-off between delivery speed and structural safety during reconstruction. Area designations under the transformation law [45] worked with zoning provisions and municipal statutes [41, 43, 44] to move density away from fault-parallel fills, liquefaction-prone ground, active landslide zones, and recurrent floodplains, while reserving corridors for emergency access through districts that would otherwise close under the weight of well-intentioned building fronts. Debris management was treated as time-bound. Sites were selected, capacities and controls documented, and decommissioning scheduled so extraordinary uses did not become normal. Delivery and inspection advanced together as the baseline for clearance workload and its spatial heterogeneity.

Public housing and rural programs moved in parallel with on-site rebuilding, but in every case, occupancy relied on the same chain of approvals and evidence. Inspection resources became consequential at the municipal level [42]. Ratios of inspectors to active units had to be set in advance and audited monthly; otherwise headline output would mask a quality deficit that surfaces under the next shock. If reconstruction is read only as counts, speed will be rewarded even when it accumulates latent risk; if it is read as the production of safe, inspected, and serviced homes, quality and pace become a single obligation. The panel regression finding in Section 3.4, that high-damage provinces show lower pace ($\beta = -0.041$) even under province and month fixed effects, reinforces this observation: where damage is most severe, the inspection and preparation workload is correspondingly heavier, and honest reporting of pace requires explicit attention to the quality gates those workloads represent.

Conditions during debris clearance and selective demolition are documented in Figure 14. Mixed debris fields contiguous with partly occupied blocks require fenced exclusion zones, dust suppression, and controlled haul-route access to protect residents and circulating school and clinic traffic. Partially overturned reinforced-concrete frames with rooftop equipment necessitate prior utility isolation, remote cutting, and crane staging rather than ground-level pulling. Mechanical demolition in constrained streets with pooled surface water and fines requires wheel-wash, leachate and silt control, and firm working platforms to avoid subgrade damage. Across all settings, salvage and hazardous-material segregation should precede bulk removal, and volumes, haul routes, and tipping sites should be logged against a dated decommissioning note so temporary uses do not become permanent. Sequencing of these measures is experienced by households as quieter windows, cleaner air, safer walking routes, and predictable access to services while reconstruction proceeds.

Figure 14. Debris clearance and selective demolition in dense urban fabric: (a) mixed debris fields adjacent to occupied blocks; (b) partially overturned reinforced-concrete frame with rooftop equipment; (c) mechanical demolition and haul-off along a constrained street.

Environmental and social safeguards moved from guidance to contractual infrastructure [57]. Site-level plans specified noise and dust control, haul routes, waste handling, and grievance redress; compliance was verified at milestones, and complaints were logged and closed on published timelines. These devices protect neighborhoods under stress, prevent nuisance burdens from shifting to those with the least voice, and preserve the legitimacy of programs that must operate for years rather than weeks.

Lifelines progressed from emergency patching to structured redundancy [31, 33]. Early intelligence highlighted corridor weaknesses, and plans began to include measures checkable on paper and on the ground: looping trunk mains, sectionalizing valves, paired substations, and reservations for emergency public space. The near-term effect was shorter interruptions during work; the long-term effect was the avoidance of single-point failures that would otherwise force large-scale sheltering. Energy and water utilities report that pairing upgrades and drawing sectionalization maps paid for themselves in the first heat wave and the first heavy rain. Where program focus narrowed to housing counts, post-occupancy projects now seek to graft redundancy onto networks not designed for them. Infrastructure and service tables record these decisions with the granularity required for audit.

Procurement and supply chains set the pace in quieter ways. Award data and change orders posted on a fixed calendar discouraged opportunistic substitutions [23]. Materials testing for steel, cement, and aggregates, coupled with laboratory access for smaller contractors, allowed supervision to shift from paperwork to workmanship. Transport lead times for mechanical and electrical assemblies constrained sequencing in several corridors. Municipalities that staged infrastructure contracts in parallel with housing and pre-positioned warehousing for pipes, transformers, and switchgear reached handover with fewer post-occupancy interruptions. These mechanics are intentionally unremarkable, which is precisely what makes them durable.

4.6. Governance Implications and Diagnostic Application

Three governance implications follow from reading the diagnostic results in Section 3 alongside the implementation narrative in Sections 4.1 through 4.5. The alignment and pace diagnostics are operationally coupled yet analytically separable. The moderate Theil divergence of 0.087 coexists with heterogeneous pace trajectories across the corridor because alignment is determined predominantly at the program-design stage, whereas pace is conditioned by the municipal gates through which entitlements are converted into handed-over units. A province may be over-allocated relative to its need share while simultaneously recording a below-average mean delivery pace of 0.774, a combination attributable to the scale and complexity of its reconstruction portfolio. Under-allocation and persistent pace shortfalls may equally coincide, as documented for Adıyaman at −6.0 percentage points, where compound constraints on both the resource and delivery dimensions are identified. These co-occurrences are expected outcomes of a system in which equity and speed are governed by distinct institutional levers, rather than anomalies, which reinforces the case for their separate and continuous monitoring.

The compositional analysis carries implications that extend beyond descriptive taxonomy. The provincial clusters identified through the Jensen–Shannon divergence structure in Tables 4 and 5 face qualitatively similar reconstruction challenges, and the intensity ratios in Table 6 quantify how commercial and agricultural workloads scale with the residential denominator. Where portfolios are compositionally close, implementation experience is transferable with only scale-related adjustments; where they are compositionally distinct, tailored combinations of housing, workplace and rural-livelihood interventions are required. This observation is particularly relevant for regional coordination bodies and for international assistance programs in which operational expertise tends to be organized along sectoral rather than territorial lines [30–35].

The panel regression reported in Section 3.4 provides an early quantitative anchor for the claim that delivery pace reflects the interaction of physical damage severity with urban form and accessibility. The negative damage–pace coefficient of −0.041 and the positive Phase 2 interaction of +0.052 together describe a system in which initial delivery is suppressed where damage is densest but in which the gap closes progressively as mobilization is completed and production is scaled. An important implication for contingency planning follows. Headline pace metrics recorded during the first year of reconstruction systematically under-represent long-run delivery capacity in the hardest-hit provinces, and reporting conventions should therefore distinguish mobilization-phase performance from steady-state delivery. The run rule adopted in this study [28] is one such convention; complementary rolling-window thresholds could support routine administrative disclosure in parallel.

The diagnostics proposed in this paper are designed to operate within existing institutional systems rather than alongside them. The DAA index functions as a corridor-scale equity instrument: where divergence is elevated, targeted adjustments in entitlements, temporary settlement capacity, or supporting infrastructure may be warranted. Sustained sequences of low RPI values trigger focused reviews of permitting throughput, inspection capacity, and utility readiness, enabling resources to be surged or delivery plans rephased where bottlenecks emerge. The reliance of both metrics on administrative ledgers already produced as part of routine government operations is a deliberate design choice, intended to minimize implementation friction and to permit external audits without the need for a parallel monitoring architecture.

Cross-regional comparability depends on the uniform quality of the administrative ledgers that populate both diagnostics. Inter-provincial variation in tagging speed, appeals density and inspection lag can propagate into the diagnostic outputs in asymmetric ways. For the Damage–Aid Alignment, revisions to building classifications after the initial sweep alter the need share s_i^{need} and hence the divergence measure; the province-level bootstrap reported above captures the sensitivity of the ranking statistics to sample composition but does not fully absorb within-province reclassification noise, which remains a residual source of uncertainty. For the Reconstruction Pace Index, differences in the cadence at which municipal offices log deliveries against plans introduce within-province noise, which the pre-specified run rule filters by requiring two consecutive months of shortfall before a warning is issued. The remaining risk is that systematic under-reporting in a given province produces biased rather than merely noisy estimates. This risk is mitigated by cross-checking the administrative series against Copernicus and ARIA products, which are in high agreement with the administrative accounts in the four most affected provinces and diverge in peripheral areas where inspection lags extended beyond six weeks. A conservative reading is therefore recommended in jurisdictions where ledger updates lag field conditions by more than approximately six weeks, and external audit should extend to input-quality review rather than output figures alone.

A practical implementation pathway is available to any municipality or provincial authority that wishes to apply the diagnostics within its existing reporting architecture, and six steps are required. First, the administrative damage ledger is aggregated at province–month resolution, and severity categories are harmonized to the collapsed, urgently demolishable, and heavily damaged counts used here. Second, the pre-event resident population is drawn from the most recent address-based register, and the Damage Severity Index is computed for each province. Third, housing entitlement allocations and related instruments are compiled on the same time base, and need and allocation shares are derived. Fourth, the damage–aid alignment statistics, namely Spearman's rank correlation and the Theil T divergence, are computed together with province-level bootstrap intervals. Fifth, the rolling monthly plan and the recorded deliveries are entered into the Reconstruction Pace Index; out-of-denominator and not-applicable cases are flagged according to the pre-specified rules; and the run condition is applied to identify persistent shortfalls. Sixth, the outputs are published alongside the input ledgers at a defined reporting cadence, which permits internal review by the municipal department and external audit by independent parties. Since each step draws on records that the municipality already produces for statutory purposes, the additional institutional cost is limited to the analytical procedure and the disclosure template, and no parallel data collection is required.

The municipal gates operate through four identifiable mechanisms that jointly account for the panel-regression signs. Plan revision is the first. Where severe damage coincides with dense, heritage-sensitive urban fabric, the statutory procedure under Law No. 3194 and Law No. 6306 extends the interval between entitlement adjudication and parcel-level construction, as exemplified in Hatay and captured by the negative damage-severity coefficient ($\beta = -0.041$). Permitting and inspection throughput follows as the second. Urban portfolios compress parcel documentation, scheduling, and approvals within a compact geographic footprint, allowing municipal departments to resource recurring workloads in advance, a scaling effect captured by the positive urban-share coefficient ($\beta = +0.033$) and visible in the sustained above-plan performance of Gaziantep, Kahramanmaraş, and Osmaniye (mean RPI 1.050, 0.969, and 1.004). Site-preparation logistics in dispersed-site portfolios operate in the opposite direction. In Adıyaman and Elazığ, travel between rural parcels and prerequisite works such as access roads and foundation excavation lengthen the permit-to-acceptance interval, an effect captured by the positive accessibility coefficient ($\beta = +0.026$) and expressed as the run-rule triggers recorded in these two provinces during August–October 2023, with convergence toward corridor-average performance by the fourth quarter. Utility energization at handover closes the sequence. Sequential commissioning of electricity, water, and wastewater connections is routinely the rate-limiting step, and the positive Phase 2 interaction between damage severity and pace ($\beta = +0.052$) is consistent with the cumulative buildup of energized capacity that allows high-damage provinces to close the delivery gap inherited from mobilization.

When these mechanisms are considered jointly, municipal gates are shown to be specific administrative processes with measurable sub-steps rather than abstract categories, with each sub-step acting as the proximate constraint on throughput that the panel-regression coefficients aggregate. The analysis remains descriptive in the sense set out in Section 2.6, and sharper interpretation would require gate-level microdata on permit-submission, inspection-completion, energization, and beneficiary-transfer dates, which would permit direct estimation of the waiting time at each sub-step and convert the four pathways from interpretive mechanisms into measured process flows.

4.7. Comparison with Prior Findings

The diagnostic results reported in the preceding sections acquire their full significance when positioned against the empirical record of recent large-scale post-earthquake recoveries. A structured comparison is presented below along the four principal dimensions of the analysis, namely proportionality, net provincial departures, pace, and conditional associations, with the explicit recognition that the resolution at which equity and pace are read in this study introduces features that are not commonly reported in the existing literature.

The strong rank correlation of $\rho_s = 0.836$ between population-normalized damage and recorded allocations is consistent with the nationwide evidence assembled for United States federal disaster programs, where post-disaster grants have been shown to be largely driven by recent disaster damage across approximately three thousand counties over a multi-year panel [80]. Broad proportionality between measured damage and distributed aid has likewise been documented in comparative work on post-disaster assistance distribution at national scale [81]. The complementary Theil T divergence of 0.087 is one of the less commonly reported statistics in the post-earthquake recovery literature at province scale, and its interpretation is anchored to the information-theoretic scale on which the measure is defined rather than to an external benchmark. A value approaching zero indicates proportionality to need, whereas values approaching the upper end of the scale reflect severely concentrated allocation. The magnitude observed here is therefore interpreted as broadly proportional with meaningful but bounded departures, a reading that is consistent with the qualitative observation in comparative studies that aid-to-damage ratios are typically highly variable across affected jurisdictions [82]. Methodologically, the use of a decomposable, entropy-based inequality measure follows the precedent of Theil-based spatial analyses in the Turkish regional-development literature [83] and of recent applications in infrastructure-resilience measurement [84], which have similarly recommended information-theoretic divergence measures over single-point statistics such as the Gini coefficient. The joint adoption of Spearman's rank correlation and the Theil T divergence, reported together at province–month resolution, is a methodological extension relative to prior post-earthquake studies, which have typically reported either ordinal or cardinal inequality measures in isolation.

The asymmetric net departures between Hatay, at +10.4 percentage points above need, and Adıyaman, at −6.0 percentage points below need, reproduce a pattern previously documented in comparative studies of Turkish post-earthquake reconstruction. Earlier work on the 1999 Marmara earthquake reconstruction program identified systematic over-allocation to provinces with concentrated urban damage and complex reconstruction portfolios, together with under-allocation to smaller provinces with more limited local implementation capacity [26]. Platt & So [27] observe more generally, in comparative analyses of post-disaster recoveries in Japan, Türkiye, and Chile, that the trade-off between speed and deliberation shapes allocation pathways in ways that predictably favor larger, urban-dominant affected areas. The provincial departures reported in this study are therefore interpretable not as idiosyncratic features of the 2023 corridor but as the renewed expression of a structural pattern that has been repeatedly observed in Turkish and comparative post-earthquake settings. Complementary findings on the same event have been reported by Galasso & Opabola [85], whose qualitative assessment of the 2023 sequence highlights the importance of quality assurance and community-led reconstruction; that study and the present analysis address different dimensions of recovery performance, namely construction quality on the one hand and allocation–delivery diagnostics on the other, and are best read as complementary rather than overlapping contributions.

The pace-diagnostic result, in which three provinces trigger the pre-specified run rule but all return to above-threshold performance within approximately two months, requires interpretation against the institutional points of departure of the compared settings rather than against their delivery rates in isolation. Following the 2015 Gorkha earthquake, the Nepalese National Reconstruction Authority was established eight months after the disaster and began signing grant agreements with beneficiaries a further four months later; approximately four years after the event, independent assessments reported that roughly 46 percent of affected households had rebuilt, a trajectory shaped by a concurrent federal constitutional transition, grant-disbursement procedures organized in multiple tranches, and recurrent staffing changes within the reconstruction authority [86]. In Canterbury, the central-city anchor-project program experienced extended delivery horizons, with the majority of anchor projects falling behind their originally scheduled completion dates as the Canterbury Earthquake Recovery Authority and the Christchurch City Council worked through institutional coordination challenges [24]. The comparatively rapid re-entry to above-threshold performance observed in the 2023 Türkiye corridor reflects different institutional preconditions, in particular the pre-existing delivery architecture of TOKİ and Emlak GYO and the parallel on-site rebuild instrument of Yerinde Dönüşüm, rather than an intrinsic superiority of one program over another. Read in this way, the RPI run-rule pattern is interpreted as evidence that early-phase shortfalls in the Türkiye corridor reflect mobilization frictions operating on a mature delivery backbone, whereas the Nepal and Canterbury trajectories reflect the additional time required to construct the delivery backbone itself.

The panel-regression coefficients, namely a damage-severity effect of $\beta = -0.041$ on pace, an urban-share effect of $\beta = +0.033$, an accessibility effect of $\beta = +0.026$, and a Phase 2 damage-severity interaction of $\beta = +0.052$, reproduce at province–month resolution the directional relationships identified qualitatively in recent comparative reconstruction studies. Governance-oriented analyses of the Canterbury [24] and Great East Japan [25] sequences have consistently reported that severely damaged jurisdictions exhibit slower early-phase delivery, that urban form conditions the pace at which routinized administrative workloads are processed, and that access constraints shape the spatial pattern of recovery. The present study quantifies these associations with explicit signs, magnitudes, and significance levels under province and month fixed effects. The correspondence between the qualitative observations reported in the comparative literature and the panel estimates obtained here strengthens the external validity of the proposed diagnostics and supports the expectation that DAA and RPI are likely to reproduce interpretable patterns in other post-earthquake settings, subject to the caveat that administrative ledger quality and planning-baseline conventions vary across institutional contexts.

5. Conclusion

This study offered an integrated reading of post-earthquake recovery in the eleven Turkish provinces struck by the 2023 Kahramanmaraş doublet, combining a corridor-level framing of the event, a close account of how temporary settlements and reconstruction programs were organized, and two quantitative, rule-based diagnostics, the Damage–Aid Alignment index (DAA) and the Reconstruction Pace Index (RPI), developed and applied at province-by-month resolution. An author-compiled, harmonized building-level corpus of 15,928 records was constructed, cross-checked against Copernicus Emergency Management Service graded-damage products and NASA ARIA displacement fields, and aggregated to a province–month panel spanning March 2023 to August 2024. The compositional layer of the analysis summarized sample shares with Wilson 95% confidence intervals, compared provincial mixes with Jensen–Shannon divergence and Dirichlet–Laplace-smoothed distributions, quantified commercial and agricultural intensities relative to residential counts, and fitted a log–log relation between commercial and residential damage.

Four empirical findings carry the argument. First, Spearman's rank correlation between population-normalized need and housing entitlement allocations is $\rho_s = 0.836$ ($p = 0.001$, 95% bootstrap CI [0.402, 0.991]), and the Theil T divergence is 0.087 (95% CI [0.031, 0.174]). Recovery effort is thus broadly proportional to measured need, although the departures from strict proportionality are statistically distinguishable from sampling variation and economically meaningful. Second, departures concentrate in interpretable ways: Hatay's allocation share exceeds its need share by 10.4 percentage points, consistent with the scale and program mix of its reconstruction portfolio, whereas Adıyaman is under-allocated by 6.0 percentage points. Third, persistent under-delivery is confined to three provinces, Adıyaman, Elazığ, and Kilis, whose pace trajectories trigger the run rule in the pre-specified interval [0.20, 0.33]. Elsewhere, monthly pace recovers within one to two months of the early-warning onset, indicating that the flagged shortfalls reflect mobilization-phase frictions rather than sustained systemic failure. Fourth, the two-way fixed-effects panel regression shows that pre-event damage severity suppresses pace ($\beta = -0.041$, $p = 0.013$), whereas urban share ($\beta = +0.033$) and site accessibility ($\beta = +0.026$) exert positive associations. The Phase 2 interaction with damage severity ($\beta = +0.052$) indicates that the initial pace gap narrows as mobilization completes.

Three broader contributions follow. First, DAA and RPI make post-disaster performance auditable without requiring bespoke data systems: both are constructed from standard administrative ledgers and interpreted against the legally codified municipal gates of siting, plan revision, permitting, inspection, and energization. Second, the compositional analysis clarifies that provinces with similar damage totals can face very different administrative burdens depending on the mix of dwellings, commercial premises, and barns; this implies that regional coordination is enhanced when provinces with compositionally close portfolios exchange implementation playbooks, whereas compositionally distinct provinces are recognized as requiring tailored interventions. Third, the framework reframes recovery as a measurable governance outcome: measurement, financing, and implementation are not parallel processes but a single legal chain, and diagnostic readings are most informative when they are anchored to that chain rather than to descriptive completion ratios.

Three limitations are recognized and bear directly on how the findings should be interpreted and extended. The corpus is an observed administrative sample rather than a census; although harmonization with humanitarian aggregation products and cross-checks against Copernicus and ARIA layers mitigate this, the statistics describe records rather than the full population of damaged structures and appeals and revisions may reallocate counts across categories and months after the data cut-off. The panel is descriptive: coefficients are interpreted as conditional associations, not as causal effects, since allocations and pace are the outcomes of non-random policy processes, and credible quasi-experimental variation is not available in this setting. The eighteen-month window captures mobilization and the transition to steady-state delivery but does not cover the medium-run outcomes of occupancy, post-handover quality and long-run equity of outcomes; these are observable only in later phases and require a continuation of the same monitoring architecture.

Four lines of further work follow directly. First, extending the panel to include post-handover periods would allow evaluation of occupancy patterns, building performance in subsequent shocks, and the long-run alignment between reconstruction investments and realized well-being. Second, integrating inspection logs and post-occupancy surveys into the RPI denominator would permit the framework to distinguish output from quality-adjusted output, addressing the central concern that pace reported without quality can reward speed at the expense of safety. Third, exporting the diagnostic architecture to other post-earthquake settings would test the generality of the thresholds and run rules proposed here and inform their calibration across institutional contexts. Fourth, credible causal identification, through instrumental-variable, regression-discontinuity, or staggered-adoption designs built on variation in transfer rules or funding formulas, would allow the panel estimates to be upgraded from structured descriptions of conditional associations to impact estimates, strengthening the evidence base for policy recommendations.

Whether reconstruction reduces risk or reproduces it will depend on routine governance habits, honest measurement, auditable pace, proportional allocation, and integrated delivery, exercised over years rather than months. The diagnostics introduced in this paper aim to make those habits legible, comparable across provinces and time, and usable inside the existing institutional framework. Recovery is not a single decision, and it is not complete until ordinary life is legible again: children walk to school along predictable routes, buses run on known timetables, workshops reopen on old corners, and the fabric of neighborhoods absorbs the rhythm of daily commerce. The 2023 sequence generated an unprecedented administrative and physical task in Türkiye, and the scale of that task will remain the reference for disaster governance research and practice for some time. By making equity and pace measurable in standard administrative units, the approach advanced here is offered as a contribution to the ordinary infrastructure of that measurement to support reconstruction that is recognizably both fair and timely.

6. Declarations

6.1. Author Contributions

Conceptualization, E.O. and R.O.; methodology, R.O.; software, E.O.; validation R.O.; investigation, E.O.; data curation, R.O.; writing—original draft preparation E.O.; writing—review and editing, R.O.; visualization, E.O.; supervision, R.O.; funding acquisition, R.O. All authors have read and agreed to the published version of the manuscript.

6.2. Data Availability Statement

The data presented in this study are available on request from the corresponding author.

6.3. Funding

This study was generously supported by funding from The Scientific and Technological Research Institution of Türkiye (TÜBİTAK) under the “1002-C Natural Disasters-Focused Fieldwork Emergency Support Program” with a Project ID: 123D071.

6.4. Conflicts of Interest

The authors declare no conflict of interest.

7. References

[1] AFAD. (2023). 06 February 2023 Pazarcık (Kahramanmaraş) Mw 7.7 and Elbistan (Kahramanmaraş) Mw 7.6 Earthquakes Preliminary Assessment Report. Ministry of Interior, Disaster and Emergency Management Presidency (AFAD), Ankara, Türkiye.

[2] TBDY-2018. (2018). Türkiye Building Earthquake Code. Ministry of Environment, Urbanization and Climate Change, Ankara, Türkiye.

[3] Cetin, K. O, Ilgac, M., & Cakir, E. (2023). Preliminary Reconnaissance Report on February 6, 2023, Pazarcik Mw=7.7 and Elbistan Mw=7.6, Kahramanmaras–Turkiye Earthquakes. Report No. 23/01, Earthquake Engineering Research Center (METU/EERC), Middle East Technical University, Ankara, Türkiye.

[4] He, L., Feng, G., Xu, W., Wang, Y., Xiong, Z., Gao, H., & Liu, X. (2023). Coseismic Kinematics of the 2023 Kahramanmaras, Turkey Earthquake Sequence from InSAR and Optical Data. Geophysical Research Letters, 50(17), 2023 104693. doi:10.1029/2023GL104693.

[5] Barbot, S., Luo, H., Wang, T., Hamiel, Y., Piatibratova, O., Javed, M. T., Braitenberg, C., & Gurbuz, G. (2023). Slip distribution of the February 6, 2023 Mw 7.8 and Mw 7.6, Kahramanmaraş, Turkey earthquake sequence in the East Anatolian Fault Zone. Seismica, 2(3). doi:10.26443/seismica.v2i3.502.

[6] Jia, Z., Jin, Z., Marchandon, M., Ulrich, T., Gabriel, A. A., Fan, W., Shearer, P., Zou, X., Rekoske, J., Bulut, F., Garagon, A., & Fialko, Y. (2023). The complex dynamics of the 2023 Kahramanmaras, Turkey, Mw 7.8-7.7 earthquake doublet. Science, 381(6661), 985–990. doi:10.1126/science.adi0685.

[7] Gokceoglu, C. (2023). 6 February 2023 Kahramanmaraş – Türkiye Earthquakes: A General Overview. The International Archives of the Photogrammetry, Remote Sensing and Spatial Information Sciences, XLVIII-M-1-2023, 417–424. doi:10.5194/isprs-archives-xlviii-m-1-2023-417-2023.

[8] Kobayashi, T., Munekane, H., Kuwahara, M., & Furui, H. (2023). Insights on the 2023 Kahramanmaraş Earthquake, Turkey, from InSAR: fault locations, rupture styles and induced deformation. Geophysical Journal International, 236(2), 1068–1088. doi:10.1093/gji/ggad464.

[9] Reitman, N. G., Briggs, R., Barnhart, W. D., Jobe, J. A., Duross, C. B., Hatem, A. E., Gold, R. D., Akçiz, S., Koehler, R., DMejstrik, J. D., & Akçiz, J. (2024). Fault Rupture Mapping of the 6 February 2023 Kahramanmaraş, Türkiye, Earthquake Sequence from Satellite Data. U.S. Geological Survey Data Release, Reston, Virginia. doi:10.5066/P985I7U2.

[10] Copernicus Emergency Management Service. (2023). EMSR648: Earthquakes in Türkiye — Activation Overview. European Commission Joint Research Centre, Brussels, Belgium. Available online: https://emergency.copernicus.eu/mapping/list-of-components/EMSR648 (accessed on April 2026).

[11] Yun, S. H., Hudnut, K., Owen, S., Webb, F., Simons, M., Sacco, P., Gurrola, E., Manipon, G., Liang, C., Fielding, E., Milillo, P., Hua, H., & Coletta, A. (2015). Rapid damage mapping for the 2015 Mw 7.8 Gorkha Earthquake Using synthetic aperture radar data from COSMO-SkyMed and ALOS-2 satellites. Seismological Research Letters, 86(6), 1549–1556. doi:10.1785/0220150152.

[12] NASA-JPL Advanced Rapid Imaging and Analysis (ARIA). (2023). Damage Proxy Map and Displacement Products for the February 2023 Türkiye–Syria Earthquakes. NASA Jet Propulsion Laboratory, Washington, United States. Available online: https://aria.jpl.nasa.gov (accessed on April 2026).

[13] Ferrentino, E., Nunziata, F., Buono, A., Urciuoli, A., & Migliaccio, M. (2020). Multipolarization Time Series of Sentinel-1 SAR Imagery to Analyze Variations of Reservoirs' Water Body. IEEE Journal of Selected Topics in Applied Earth Observations and Remote Sensing, 13, 840–846. doi:10.1109/JSTARS.2019.2961563.

[14] Jung, J., & Yun, S. H. (2020). Evaluation of coherent and incoherent landslide detection methods based on synthetic aperture radar for rapid response: A case study for the 2018 Hokkaido landslides. Remote Sensing, 12(2), 265. doi:10.3390/rs12020265.

[15] Strategy and Budget Office of the Presidency of the Republic of Türkiye. (2024). 2023 Kahramanmaraş and Hatay Earthquakes Report (Türkiye Earthquakes Recovery and Reconstruction Assessment — TERRA). Presidency of the Republic of Türkiye, Ankara, Türkiye. Available online: https://www.sbb.gov.tr (accessed on April 2026).

[16] Apostolaki, S., Riga, E., & Pitilakis, D. (2024). Rapid damage assessment effectiveness for the 2023 Kahramanmaraş Türkiye earthquake sequence. International Journal of Disaster Risk Reduction, 111, 104691. doi:10.1016/j.ijdrr.2024.104691.

[17] Brown, D., Saito, K., Spence, R., Chenvidyakarn, T., Adams, B., Mcmillan, A., & Platt, S. (2008). Indicators for measuring, monitoring and evaluating post-disaster recovery. Proceedings 6th International Workshop on Remote Sensing for Disaster App, 11-12 September, 2008, Pavia, Italy.

[18] Horney, J., Dwyer, C., Aminto, M., Berke, P., & Smith, G. (2017). Developing indicators to measure post-disaster community recovery in the United States. Disasters, 41(1), 124–149. doi:10.1111/disa.12190.

[19] Geiß, C., & Taubenböck, H. (2013). Remote sensing contributing to assess earthquake risk: From a literature review towards a roadmap. Natural Hazards, 68(1), 7–48. doi:10.1007/s11069-012-0322-2.

[20] Ghaffarian, S., Kerle, N., & Filatova, T. (2018). Remote sensing-based proxies for urban disaster risk management and resilience: A review. Remote Sensing, 10(11), 1760. doi:10.3390/rs10111760.

[21] Dell'Acqua, F., & Gamba, P. (2012). Remote sensing and earthquake damage assessment: Experiences, limits, and perspectives. Proceedings of the IEEE, 100(10), 2876–2890. doi:10.1109/JPROC.2012.2196404.

[22] Altaie, M. R., Dishar, M. M., & Muhsin, I. F. (2023). Fundamental Challenges and Management Opportunities in Post Disaster Reconstruction Project. Civil Engineering Journal, 9(9), 2161–2174. doi:10.28991/CEJ-2023-09-09-05.

[23] Bakr, E. H., Elbeltagi, E., & Tantawy, M. (2025). BIM Utilization to Eliminate Claims, Risks, and Improve Productivity in Construction Projects. Civil Engineering Journal, 11(12), 5100–5131. doi:10.28991/CEJ-2025-011-12-011.

[24] Johnson, L. A., & Mamula-Seadon, L. (2014). Transforming governance: How national policies and organizations for managing disaster recovery evolved following the 4 September 2010 and 22 February 2011 Canterbury earthquakes. Earthquake Spectra, 30(1), 577–605. doi:10.1193/032513EQS078M.

[25] Cho, A. (2014). Post-tsunami recovery and reconstruction: governance issues and implications of the Great East Japan Earthquake. Disasters, 38(s2), 157-178. doi:10.1111/disa.12068.

[26] Ganapati, N. E., & Ganapati, S. (2008). Enabling Participatory Planning After Disasters: A Case Study of the World Bank's Housing Reconstruction in Turkey. Journal of the American Planning Association, 75(1), 41–59. doi:10.1080/01944360802546254.

[27] Platt, S., & So, E. (2017). Speed or deliberation: a comparison of post-disaster recovery in Japan, Turkey, and Chile. Disasters, 41(4), 696–727. doi:10.1111/disa.12219.

[28] Montgomery, D. C. (2020). Introduction to statistical quality control. John Wiley & Sons, Hoboken, United States.

[29] AFAD. (2022). Türkiye Disaster Response Plan (TAMP). Disaster and Emergency Management Presidency, Republic of Türkiye, Ministry of Interior, Ankara, Türkiye.

[30] Kim, K., & Olshansky, R. B. (2014). The theory and practice of building back better. Journal of the American Planning Association, 80(4), 289–292. doi:10.1080/01944363.2014.988597.

[31] El Hage, J., Shahrour, I., Hage Chehade, F., & Abi Farraj, F. (2023). A comprehensive assessment of buildings for post-disaster sustainable reconstruction: A case study of Beirut Port. Sustainability, 15(18), 13433. doi:10.3390/su151813433.

[32] Murakami, K., Wood, D. M., Tomita, H., Miyake, S., Shiraki, R., Murakami, K., ... & Dimmer, C. (2014). Planning innovation and post-disaster reconstruction: The case of Tohoku, Japan/Reconstruction of tsunami-devastated fishing villages in the Tohoku region of Japan and the challenges for planning/Post-disaster reconstruction in Iwate and new planning challenges for Japan/Towards a "network community" for the displaced town of Namie, FukushimaResilience design and community support in Iitate Village in the aftermath of the Fukushima Daiichi nuclear disaster/Evolving place governance innovations and .... Planning Theory & Practice, 15(2), 237-242. doi:10.1080/14649357.2014.902909.

[33] Tian, R., Zhang, Y., Peng, L., Wang, Y., Wang, W., & Gu, Y. (2024). Measurement of flood resilience of metro station based on combination weighting-cloud model. International Journal of Disaster Risk Reduction, 114, 104950. doi:10.1016/j.ijdrr.2024.104950.

[34] Ge, Y., Gu, Y., & Deng, W. (2010). Evaluating China's national post-disaster plans: The 2008 Wenchuan earthquake's recovery and reconstruction planning. International Journal of Disaster Risk Science, 1(2), 17-27. doi:10.3974/j.issn.2095-0055.2010.02.003.

[35] Li, X., Yu, H., Xu, H., Ren, X., Song, W., & Zhang, J. (2023). A comparative study on pedestrian flow through bottlenecks between flood evacuation and land evacuation. International Journal of Disaster Risk Reduction, 95, 103822. doi:10.1016/j.ijdrr.2023.103822.

[36] Mochizuki, J., & Chang, S. E. (2017). Disasters as opportunity for change: Tsunami recovery and energy transition in Japan. International Journal of Disaster Risk Reduction, 21, 331–339. doi:10.1016/j.ijdrr.2017.01.009.

[37] Mulligan, M., Steele, W., Rickards, L., & Fünfgeld, H. (2016). Keywords in planning: what do we mean by 'community resilience'? International Planning Studies, 21(4), 348–361. doi:10.1080/13563475.2016.1155974.

[38] Dunz, N., Tanaka, H., Shiiba, N., Mochizuki, J., & Naqvi, S. A. A. (2021). Building back better in small Island developing states in the pacific: Initial insights from the bind model of disaster risk management policy options in Fiji. ADBI Working Paper, 1290.

[39] Emre, Ö., Duman, T. Y., Özalp, S., Şaroğlu, F., Olgun, Ş., Elmacı, H., & Çan, T. (2018). Active fault database of Turkey. Bulletin of Earthquake Engineering, 16(8), 3229–3275. doi:10.1007/s10518-016-0041-2.

[40] Oyguc, R. (2016). Seismic performance of RC school buildings after 2011 Van earthquakes. Bulletin of Earthquake Engineering, 14(3), 821–847. doi:10.1007/s10518-015-9857-4.

[41] Official Gazette No. 18749. (1985). Construction Zoning Law No. 3194. Republic of Türkiye, Ankara, Türkiye.

[42] Official Gazette No. 24461. (2001). Building Inspection Law No. 4708. Republic of Türkiye, Ankara, Türkiye.

[43] Official Gazette No. 25874. (2005). Municipal Law No. 5393. Republic of Türkiye, Ankara, Türkiye.

[44] Official Gazette No. 25531. (2004). Metropolitan Municipality Law No. 5216. Republic of Türkiye, Ankara, Türkiye.

[45] Official Gazette No. 28309. (2012). Law No. 6306 on the Transformation of Areas Under Disaster Risk. Republic of Türkiye, Ankara, Türkiye.

[46] Official Gazette No. 27261. (2009). Law No. 5902 on the Organisation and Duties of the Disaster and Emergency Management Presidency. Republic of Türkiye, Ankara, Türkiye.

[47] Şevkin, E., & Gül, M. (2025). Local government reform in Turkey and its aftermath: the urban transformation of Istanbul between 1984 and 1989. Middle Eastern Studies, 61(4), 474-487. doi:10.1080/00263206.2024.2431008.

[48] McCormick, K., Anderberg, S., Coenen, L., & Neij, L. (2013). Advancing sustainable urban transformation. Journal of Cleaner Production, 50, 1–11. doi:10.1016/j.jclepro.2013.01.003.

[49] Peter, B. (2008). Urban Transformation: Understanding City Design and Form. Island Press, Washington, United States.

[50] Grandin, J., Haarstad, H., Kjærås, K., & Bouzarovski, S. (2018). The politics of rapid urban transformation. Current Opinion in Environmental Sustainability, 31, 16–22. doi:10.1016/j.cosust.2017.12.002.

[51] Montgomery, M. R. (2008). The urban transformation of the developing world. Science, 319(5864), 761–764. doi:10.1126/science.1153012.

[52] Elicin, Y. (2014). Neoliberal transformation of the Turkish city through the Urban Transformation Act. Habitat International, 41, 150–155. doi:10.1016/j.habitatint.2013.07.006.

[53] Gün, A., Pak, B., & Demir, Y. (2021). Responding to the urban transformation challenges in Turkey: a participatory design model for Istanbul. International Journal of Urban Sustainable Development, 13(1), 32-55. doi:10.1080/19463138.2020.1740707.

[54] Tek, M. (2025). Urban Transformation in Antakya Post-Earthquake Challenges and Controversies: Urban Transformation in Antakya. In Preserving Cultural Heritage in Post-Disaster Urban Renewal. IGI Global Scientific Publishing, IGI Global Scientific Publishing, United States.

[55] Saraçoğlu, C., & Demirtaş-Milz, N. (2014). Disasters as an ideological strategy for governing neoliberal urban transformation in Turkey: Insights from Izmir/Kadifekale. Disasters, 38(1), 178–201. doi:10.1111/disa.12038.

[56] Bozdağ, A., & İnam, Ş. (2021). Turkey Experience in Urban Transformation. Iconarp International J. Of Architecture and Planning, 9(2), 966–990. doi:10.15320/iconarp.2021.188.

[57] World Bank. (2015). Disaster Recovery Framework Guide. Global Facility for Disaster Reduction and Recovery (GFDRR), UNDP, and European Union, World Bank, Washington, United States.

[58] UNDRR. (2019). Global Assessment Report on Disaster Risk Reduction 2019. United Nations Office for Disaster Risk Reduction (UNDRR), Geneva, Switzerland.

[59] UNDRR. (2015). Sendai Framework for Disaster Risk Reduction 2015–2030. United Nations Office for Disaster Risk Reduction (UNDRR), Geneva, Switzerland.

[60] Al-Mosawy, S. K., Al-Jaberi, A. A., Alrobaee, T. R., & Al-Khafaji, A. S. (2021). Urban Planning and Reconstruction of Cities Post-Wars by the Approach of Events and Response Images. Civil Engineering Journal, 7(11), 1836–1852. doi:10.28991/cej-2021-03091763.

[61] IFRC. (2023). Shelter Sector Türkiye — 2023 Earthquakes Response: Situation and Response Updates. International Federation of Red Cross and Red Crescent Societies (IFRC), Shelter Cluster Türkiye, Ankara, Türkiye.

[62] Liu, C., Lay, T., Wang, R., Taymaz, T., Xie, Z., Xiong, X., Irmak, T. S., Kahraman, M., & Erman, C. (2023). Complex multi-fault rupture and triggering during the 2023 earthquake doublet in southeastern Türkiye. Nature Communications, 14(1), 5564. doi:10.1038/s41467-023-41404-5.

[63] Rodriguez-Perez, Q., & Zúñiga, F. R. (2025). Statistical and source characterization of the 2023 Kahramanmaraş Türkiye earthquake sequence. Acta Geophysica, 73(2), 1241-1260. doi:10.1007/s11600-024-01428-x.

[64] Gürboğa, Ş., Kayadibi, Ö., Akilli, H., Arikan, S., & Tan, S. (2024). Preliminary results of the great Kahramanmaraş 6 February 2023 earthquakes (MW 7.7 and 7.6) and 20 February 2023 Antakya earthquake (MW 6.4), Eastern Türkiye. Turkish Journal of Earth Sciences, 33(1), 22-39. doi:10.55730/1300-0985.1896.

[65] TÜİK. (2023). Address-Based Population Registration System Results, 2022. Turkish Statistical Institute (TÜİK), Ankara, Türkiye.

[66] Zhang, S., Tian, J., Lu, X., Tian, Q., He, S., Lin, Y., Li, S., Zheng, W., Wen, T., Mu, X., Zhang, J., & Li, Y. (2024). Monitoring of chlorophyll content in local saltwort species Suaeda salsa under water and salt stress based on the PROSAIL-D model in coastal wetland. Remote Sensing of Environment, 306, 306. doi:10.1016/j.rse.2024.114117.

[67] Spearman, C. (1904). The Proof and Measurement of Association between Two Things. The American Journal of Psychology, 15(1), 72. doi:10.2307/1412159.

[68] Kendall, M. G. (1938). A New Measure Of Rank Correlation. Biometrika, 30(1-2), 81–93. doi:10.1093/biomet/30.1-2.81.

[69] Theil, H. (1967) Economics and Information Theory. North-Holland Publishing Company, Amsterdam, Netherlands.

[70] Cowell, F. (2011). Measuring Inequality. Oxford University Press, Oxford, United Kingdom. doi:10.1093/acprof:osobl/9780199594030.001.0001.

[71] Efron, B. (1979). Bootstrap Methods: Another Look at the Jackknife. The Annals of Statistics, 7(1), 1176344552. doi:10.1214/aos/1176344552.

[72] Efron, B., & Tibshirani, R. J. (1994). An Introduction to the Bootstrap. Chapman and Hall/CRC, New York, United States. doi:10.1201/9780429246593.

[73] Colin Cameron, A., & Miller, D. L. (2015). A practitioner's guide to cluster- robust inference. Journal of Human Resources, 50(2), 317–372. doi:10.3368/jhr.50.2.317.

[74] Imai, K., & Kim, I. S. (2021). On the Use of Two-Way Fixed Effects Regression Models for Causal Inference with Panel Data. Political Analysis, 29(3), 405–415. doi:10.1017/pan.2020.33.

[75] Solveig, T., & Bartolucci, A. (2023). INSARAG Lessons Learned Summary Report: 2023 Türkiye–Syria Earthquake Response. United Nations Office for the Coordination of Humanitarian Affairs (OCHA), INSARAG Secretariat, Geneva, Switzerland.

[76] OCHA. (2023). Türkiye–Syria Earthquakes: Situation Reports Nos. 1–12. United Nations Office for the Coordination of Humanitarian Affairs (OCHA), Geneva, Switzerland.

[77] Toraman, C., Kucukkaya, I. E., Ozcelik, O., & Sahin, U. (2023). Tweets under the rubble: Detection of messages calling for help in earthquake disaster. arXiv Preprint, arXiv:2302.13403. doi:10.48550/arXiv.2302.13403.

[78] Kovancı, E. (2023). Tracing the connections between human rights and post-earthquake. Kapanaltı Dergisi, (4), 77-94.

[79] Odacı, N., Karaman, S., & Kerse, K. (2025). Container City Experiences of Nurses Providing Voluntary Health Care Services Following the Earthquake: A Qualitative Approach. Disaster Medicine and Public Health Preparedness, 19, e225. doi:10.1017/dmp.2025.10143.

[80] Miao, Q., Davlasheridze, M., & Reilly, A. C. (2025). Assessing social equity of federal disaster aid distribution: A nationwide analysis. Risk Analysis, 45(11), 3375–3395. doi:10.1111/risa.17660.

[81] Becerra, O., Cavallo, E., & Noy, I. (2014). Foreign aid in the aftermath of large natural disasters. Review of Development Economics, 18(3), 445–460. doi:10.1111/rode.12095.

[82] Waters, L., Best, K., Miao, Q., Davlasheridze, M., & Reilly, A. C. (2024). Under-reported and under-served: Disparities in US disaster federal aid-to-damage ratios after hurricanes. International Journal of Disaster Risk Reduction, 106, 104430. doi:10.1016/j.ijdrr.2024.104430.

[83] Gezici, F., & Hewings, G. J. D. (2007). Spatial analysis of regional inequalities in Turkey. European Planning Studies, 15(3), 383–403. doi:10.1080/09654310601017091.

[84] Dhakal, S., & Zhang, L. (2023). A Social Welfare–Based Infrastructure Resilience Assessment Framework: Toward Equitable Resilience for Infrastructure Development. Natural Hazards Review, 24(1), 4022042. doi:10.1061/(asce)nh.1527-6996.0000597.

[85] Galasso, C., & Opabola, E. A. (2024). The 2023 Kahramanmaraş Earthquake Sequence: finding a path to a more resilient, sustainable, and equitable society. Communications Engineering, 3(1), 24. doi:10.1038/s44172-024-00170-y.

[86] Platt, S., Gautam, D., & Rupakhety, R. (2020). Speed and quality of recovery after the Gorkha Earthquake 2015 Nepal. International Journal of Disaster Risk Reduction, 50, 101689. doi:10.1016/j.ijdrr.2020.101689.